[UCI]I804:24011-200000241928

August 2011

Ph.D. Dissertation

Influence of a Repetitive Pattern of Lysine and Tryptophan on Antimicrobial Activity and Mechanism of Action

Graduate School of Chosun University

Department of Bio-Materials

Ramamourthy Gopal

Influence of a Repetitive Pattern of Lysine and Tryptophan on Antimicrobial Activity and Mechanism of Action

라이신과 트립토판의 반복적 패턴이 항균 활성 및 항균 작용기작에 미치는 영향

25th August 2011

Graduate School of Chosun University

Department of Bio-Materials

Ramamourthy Gopal

Influence of a Repetitive Pattern of Lysine and Tryptophan on Antimicrobial Activity and Mechanism of Action

Advisor: Prof. Kyung-Soo Hahm

This dissertation is submitted to the Graduate School of the Chosun Univeristy in partial fulfillment of the requirements for the degree of Doctor of Philosophy in Science

April 2011

Graduate School of Chosun University

Department of Bio-Materials

Ramamourthy Gopal

This is to certify that the Ph.D. dissertation of Ramamourthy Gopal has successfully met the dissertation requirements of Chosun University.

Chairman	**: Prof. Song Yub Shin**	.....
Committee Member:	**Prof. Jae Il Kim**	.....
Committee Member:	**Prof. Il-Seon Park**	.....
Committee Member:	**Prof. Yoonkyung Park**	.....
Committee Member:	**Prof. Kyung-Soo Hahm**	.....

June 2011

Graduate School of Chosun University

CONTENTS

LIST OF TABLES

LIST OF FIGURES

초 록

라이신과 트립토판의 반복적 패턴이 항균 활성 및 항균 작용기작에 미치는 영향

라마모티고팔

지도교수: 함경수

생물신소재학과

조선대학교 대학원

Lysine과 Tryptophan이 많이 함유된 양이온 항균 펩타이드를 이용하여 미생물에 대한 광범위한 항균활성과 작용기작을 $(KW)_n$라는 Lysine (K) 과 Tryptophan (W)잔기가 지속적으로 포함된 일련의 scrambled 펩타이드를 합성하였고, 이들 펩타이드의 항균활성을 확인하였다. $(KW)_5$ 펩타이드를 제외하고 펩타이드 chain length의 증가에 따라 항균활성의 증가를 나타내었다. $(KW)_5$ 펩타이드는 수용성 환경에서의 self-aggregation에 의한 소수성의 증가로 세포독성 증가와 항균활성 감소를 나타냈다. 첫 번째로 박테리아 생체막에 linear 펩타이드의 효과를 연구했다. 펩타이드의 막투과 능력에 관하여 lipopolysaccharides (LPS)의 phosphate groups에 펩타이드가 강한 상호작용을 하였고, killing 활성은 막 파괴 유도와 투과 능력에 의해 빠른 붕괴를 통해 나타났다. 이후 펩타이드 활성 모드를 나타내는 것으로 Circular dichroism (CD) spectra에서 펩타이드가 수용성 용액에서

불규칙적인 구조를 나타내지만, lipid vesicles 모형에서는 β-sheet 구조 형성을 나타냈다. 또한 $(KW)_4$ 펩타이드는 주사 전자 현미경법 (SEM: scanning electron microscopy)을 이용하여 박테리아 세포에 aggregated와 박테리아 세포 표면이 파괴되는 것을 확인했다. 모든 데이터는 KW에서 변형된 긴 펩타이드로 (*n* equals 4 or 5) 박테리아 활성에 있어 aggregation되는 것을 확인하였다. 또한 이들 펩타이드의 용혈작용과 LPS 부착작용 그리고 막 투과활성은 펩타이드 길이와 소수성, 용해도에 따라서 반응의 원인이 된다는 것을 알 수 있었다.

두 번째 연구는 fungal막에 linear 펩타이드들의 효과를 나타낸 것으로 항진균 활성은 펩타이드의 길이에 따라서 증가했고, 세포 독성 또한 유사한 경향을 보였다. 펩타이드들의 최소농도 억제는 세포막 침투를 유도하지 않았지만 진균 사멸을 나타냈고, 펩타이드 활성은 세포벽 구성 요소 및 대사 억제제로 저해하지 못했다. 세포막의 변화는 세포 외부의 propidium iodide (PI)와 세포벽 사이에 축적된 calcein에 의해 평가되었다. Trp blue shift와 CD spectra를 이용한 측정은 펩타이드가 진균 막에 상호작용하는 것을 보였지만 세포투과 실험에서는 이들 펩타이드가 *Candida albicans*에 세포원형질막 투과를 유도하지 않았다. 또한 SEM을 통한 관찰에서도 $(KW)_4$ 펩타이드가 minimum inhibitory concentration (MIC)에서 세포막 형태의 변화를 일으키지 않음을 확인하였다. 덧붙여 5-carboxytetramethylrhodamine (TAMRA)를 부착한 $(KW)_4$ 펩타이드는 *Candida albicans*의 cytosol에 축적되어 위치하였다. 이들 결과들로 $(KW)_4$ 펩타이드는 진균에서 세포막의 파괴를 유도하지 않고 세포 내부로 들어가 작용하는 것으로 보였다. 이에 Gel retardation 실험을 통해 진균의 RNA에 펩타이드가 부착함을 확인하였다.

이상의 결과로부터 $(KW)_4$ 펩타이드는 박테리아 활성에 있어 aggregation되었으며, 진균에서는 세포막에 파괴를 유도하지 않고 세포 내부로 들어가 RNA에 부착됨을 알 수 있었다. 이로서 $(KW)_4$ 펩타이드는 박테리아와 진균에서 서로 다른 메커니즘으로 세포성장 억제를 유도한다는 것을 알 수 있었다.

1. Introduction

The spread of antibiotic resistance among microbial pathogens especially in hospital environments but also now in the community has occurred at an alarming rate [1,2]. There is now a proliferation of so-called "Superbugs" that are resistant to multiple antibiotics and severely limit treatment options; these include methicillin-resistant *staphylococcus aureus* (MRSA), vancomycin-resistant *enterococci* (VRE), and multi-drug-resistant *Pseudomonas aeruginosa* (MDRPA), among others, and cause hundreds of thousands of infections annually. Although, fungal infections occurs more frequently in people whose immune system is suppressed. Fungal infections are the major cause of morbidity and mortality in patients with organ transplantation, the human immunodeficiency virus (HIV) and cancer chemotherapy [3-5]. There are three main classes of clinically useful antifungal agents: polyene antibiotics, the fluoropyrimidine flucytosine, and azoles [6]. However, the toxicities of the currently used polyene antifungal drugs and the emergence of candidal species resistant to fluoropyrimidine flucytosine and azole based agents have resulted in the initiation of a search for innate peptide antibiotics as alternative drug therapies [7].

Antimicrobial peptides (AMPs) are of particular interest because their proposed mode of action does not appear to stimulate rapid development of microbial resistance [8], and over the past two decades, numerous AMPs have been identified naturally in both prokaryotes and eukaryotes, designed *de novo* and produced synthetically [9-12]. The majorities of antimicrobial peptides (AMPs) are cationic with a net charge, imparted by the presence of lysine and arginine, and contain up to 50% hydrophobic amino acids. AMPs are generally characterized by a variable in length, sequence and conformation structure (helical, beta-sheet, extended and looped) [13-15]

and exhibits broad spectrum of activity against Gram-positive and Gram-negative bacteria, fungi, parasites and viruses [14,16,17]. The amphipathicity charcteristics, rendered by cationic and hydrophobic sequence features, of AMPs allow them to bind cellular membranes of microorganisms [18-21]. Peptide-mediated cell lysis is due to the disruption of cytoplasmic membranes through several mechanisms, e.g., barrel stave, toroidal pore, or carpeting [19-21]. In the barrel-stave model [22], the amphipathic α-helical or β-sheet peptides reorient perpendicular to the membrane and align (like the staves in a barrel) in a manner in which the hydrophobic side chains face outwards into the lipid environment while the polar side chains align inward to form transmembrane pores. These pores are proposed to allow leakage of cytoplasmic components and also disrupt the membrane potential. The toroidal model (Wormwhole mechanism) differs from the barrel-stave model in that peptides are always associated with the lipid head groups even when they are perpendicular in the lipid bilayer. In the alternative carpet model [23], the peptides do not insert into the membrane but align parallel to the bilayer, remaining in contact with the lipid head groups and effectively coating the surrounding area. This orientatation leads to a local disturbance in membrane stability, causing the formation of large cracks, leakage of cytoplasimic components, disruption of the membrane potential and, ultimately, disintegration of the membrane. Also, some AMPs exert their microbicidal activities by interacting with nucleic acids, thus preventing the replication and/or transcription. On the basis of these futures, AMPs are active in preventing multidrug-resistant strains, and are thus last line of defense dealing with microbial infections. Some cationic peptides also possess anticancer [24,25] or wound healing activity [26]. Recent studies have indicated that AMPs to be able to stimulate innate immune response. Several AMPs are currently in clinical trials, mostly for topical application [27]. Although AMPs considered as an

alternative therapeutic agent, however, many AMPs are unselective between mammalian and microbial cells (e.g., pardaxin [28], melittins [29], and cathelicidins [30]. In addition, the large size of AMPs is also hindered by high manufacturing costs. Therefore, selective short AMPs have been currently developed based on their amino acid combination, charge, hydrophobicity and length [31-35].

It is well known that there are two types of amino acid side chains having a specific interaction between AMPs and polar head groups or non-polar hydrophobic core of microbial membrane: The aromatic amino acids, in particular, tryptophan (Trp) allow peptides to partition in lipid bilayer [36]. Trp side chains are commonly observed for AMPs [37-42], replacement of the three Trp residues of tritrpticin by alanine abolishes the antimicrobial activity [43], suggesting that the Trp side chain are necessary for peptide activity. The indole side chain of Trp may ensure more efficient interaction with negatively charged microbial membrane, compared with other nonpolar side chains such as phenylalanine (Phe) or tyrosine (Tyr) [41,44]. As well, many biologically active peptides analog have been developed by introduction of Trp than those with either Phe or Tyr [32,35,45].

The charged residues, arginine (Arg) and lysine (Lys) are used to present in AMPs. However, it has been shown that the side chains of Arg residues of several cationic AMPs are not selective for bacterial membranes. For example, the guanidinium group of Arg interact strongly with zwitterionic phospholipids membranes, thereby promoting eukaryotic cell toxicity. Studies reported that the replacement of Arg by Lys maintained its activity, but reduced eukaryotic toxicity [46,47]. In addition, potent AMPs are systematically designed with all Lys residues are placed on the polar face of an amphipathic structure and are proposed to interact with anionic lipid headgroups. It likely contributes to their specificity against microbes [48-

50]. Importantly, the action of many AMPs is mainly dependent on the primary sequence of the Lys [51-53]. For example, the replacement of the Lys residue in AMPs resulted in the nearly complete loss of microbicidal activity [51-53]. Also, studies of cell, internalization of Lys-rich proteins have indicated that the Lys could be essential [54]. Although it has been reported that synthetic peptides containing Lys residues bind to RNA [55] and it could be essential for peptide action in microbial cell, thus preventing cellular protein synthesis and leads to cell lead. Furthermore, synthetic cost of AMPs containing Arg is very expensive than that containing Lys.

Therefore, the clustering of these amino acids (Lys and Trp) is very responsible for antimicrobial properties. However, the effects of chain length and composition on antimicrobial activity, selectivity and mechanism of action have not been clearly investigated. Keeping these points in mind, various sizes of peptides were synthesized with alternating Lys and Trp, and determined their antimicrobial activity.

Firstly, their antibacterial and hemolytic activities were analyzed and then, their structure and organization in aqueous or model membrane were determined using circular dichroism (CD) and Trp fluorescence assay. The mechanism of antibacterial actions was investigated by various parameters, such as peptide localization, lipopolysaccharides (LPS) binding affinity, membrane depolarization, SYTOX Green uptake, time-killing assay, calcein leakage, change in vesicles size and site of peptide action. Therefore, designed scrambled peptides may be able to selectively target against bacterial membrane and exert antibacterial activity by increasing the membrane permeability, consequently cells were aggregated.

Secondly, their antifungal and cytotoxicity activities were determined. The mode of internalization of these peptides is not required cell wall components and energed cells. Here, results report that the internalization of this peptide is non lytic

membrane perturbation. However, the peptide-membrane interaction was investigated and observed by CD and fluorescence spectroscopy. Thus, it is conceivable that these peptides use their membrane binding properties so as to enter the cytoplasm and exert their antifungal activity by attacking intercellular targets other than the plasma membrane.

2. Materials and Methods

2.1. Materials

Rink amide 4-methylbenzhydrylamine resin, fluoren-9-ylmethoxycarbonyl (Fmoc) amino acids, and other reagents for the peptide synthesis were purchased from Calibochem-Novabiochem (La Jolla, CA). Acrylamide, *P. aeruginosa* LPS and sodium azide were purchased from Sigma Chemicals (St. Louis, MO). Cholesterol (CH, from porcine liver), and L-α-phosphatidylethanolamine (PE, from *E. coli*), egg yolk L-α-phosphatidylcholine (PC), L-α-phosphatidylglycerol (PG, from *E. coli*), were obtained from Avanti Polar Lipids, Co. (Alabaster, AL). Calcein, 5-carboxytetramethylrhodamine (TAMRA), 3,3'-diethylthiodicarbocyanine iodide ($DiSC_3$-5) and SYTOX Green were acquired from Molecular Probes (Eugene, OR). All other reagents were of analytical grade. Buffers were prepared using double distilled water (Millipore Co.).

Escherichia coli (KCTC 1682); *Salmonella typhimurium* (KCTC 1926); *Pseudomonas aeruginosa* (KCTC 1637); *Staphylococcus aureus* (KCTC 1621); *Bacillus subtilis* (KCTC 1918); *Listeria monocytogenes* (KCTC 3710); *Candida albicans* (KCTC 7270); *Candida catenulate* (7642); *Candida intermidia* (7234); *Candida rugosa* (7324); *Candida glabrata* (7219) and *Candida melibiosica* (KCTC 7631) were obtained from the Korean Collection for Type Cultures (KCTC). Drug-resistant *E. coli* strains (CCARM 1229 and CCARM 1238), *S. typhimurium* strains (CCARM 8007, CCARM 8009 and CCARM 8013) and *S. aureus* strains (CCARM 3108, CCARM 3089, CCARM 3126, CCARM 3090 and CCARM 3114) were obtained from the Culture Collection of Antibiotic-Resistant Microbes (CCARM) at Seoul Women's University in Korea.

2.2. Methods

2.2.1 Peptide synthesis and purification

The peptides, KWKW-NH_2 $(KW)_2$, KWKWKW-NH_2 $(KW)_3$, KWKWKWKW-NH_2 $(KW)_4$ and KWKWKWKWKW-NH_2 $(KW)_5$ were synthesized by the solid-phase method using Fmoc chemistry [56] on a solid support of rink amide 4-methylbenzhydrydrylamine resin. Peptide labeling at the N-terminus amino acid with 5-carboxytetramethylrhodamine (TAMRA) was done on the resin-bound peptide as previously described [56]. 0.1 M N-hydroxy benzotriazole (HOBt) and 0.45 M 2-(1H-benzotriazole-1-yil)-1,1,3,3-tetramethyluroniumhexafluorophosphate (HBTU) in DMF and 2 M N,N-diisopropyl ethylamine (DIEA) in N-methylpyrrolidone (NMP) were used as coupling reagent, and 10-fold excess Fmoc-amino acid were added during every coupling cycle. After final deprotection with a solution of 20% piperidine in DMF and cleavage with a mixture of TFA/water/triisopropylsilane (90:5:5) for 2 h at room temperature. The crude peptides were repeatedly extracted with diethyl ether and then purified using reverse phase preparative HPLC on a Vydac C_{18} column (4.6 x 250 mm, 300 Å, 5 nm). The molecular masses of the peptides were confirmed with a matrix-assisted laser desorption ionization mass spectrometer (MALDI II, Kratos Analytical Ins.).

2.2.2. Antibacterial activity

The antibacterial activity of the peptides against Gram-negative, Gram-positive, and ten antibiotic resistant bacteria was examined using the microbroth dilution method [58]. Aliquots of bacterial suspensions in mid-logarithmic phase at a concentration of 2 x 10^5 colony forming units (CFU)/ml in culture medium were added to each well, containing peptide solutions diluted with 2-fold serial in 10 mM sodium phosphate buffer (pH 7.2) or phosphate buffered saline (PBS, 1.5 mM KH_2PO_4, 2.7

mM KCl, 8.1 mM Na_2HPO_4, 150 mM NaCl, pH 7.2). Inhibition of growth was determined by measuring the absorbance at 620 nm, using a Versa-Max microplate Elisa Reader (Molecular Devices, Sunnyvale, CA) after incubation for 18-24 h at 37 ^oC. The minimum inhibitory concentration (MIC) is defined as the minimal peptide concentration that completely inhibits bacterial growth.

2.2.3. Antifungal activity

The fungal strains of *C. albicans* (KCTC 7270); *C. catenulate* (7642); *C. intermidia* (7234); *C. rugosa* (7324); *C. glabrata* (7219) and *C. melibiosica* (KCTC 7631) were cultured at 28 ^oC in appropriate media. Fungal cells (Final concentration 2 x 10^4 spore/ ml) that were grown in 50 µl of YPD media (yeast extract 0.5%, peptone 1%, dextrose 2%) were seeded in each well of a microtitre plate containing 50 µl of two-fold serially diluted peptides in PBS. After incubating for 24 to 30 h at 28 ^oC, the lowest concentration of the peptides inhibiting the growth of fungi was microscopically determined to be the MIC [59].

2.2.4. Hemolysis for human red blood cell (hRBC)

Hemolytic activities were assessed for peptides using heparinized hRBCs collected from healthy donors. The fresh hRBCs were washed three times in PBS (pH 7.2) via centrifugation at 800xg for 10 min and then resuspended in PBS. After washing, the peptides were dissolved in PBS and added to 100 µl of stock hRBCs suspended in PBS (final RBC concentration, 4% v/v). The samples were then incubated with gentle agitation for 60 min at 37 ^oC, after which they were centrifuged for 10 min at 800xg. The absorbance of the supernatants was recorded at 414 nm. In addition, controls for zero hemolysis (blank) and 100% hemolysis were incubated with PBS and 1% Triton X-100, respectively. Melittin was used as hemolytic peptide. Each measurement was conducted in triplicate.

2.2.5. Cell culture and cytotoxicity

To examine cytotoxic effect of peptide, HaCaT (human keratinocyte) cells were cultured in Dulbecco's modified Eagle medium (DMEM) supplemented with antibiotics (100 U/mL penicillin, 100 µg/mL streptomycin) and 10% fetal calf serum at 37 ^{o}C in a humidified chamber in an atmosphere containing 5% CO_2. The percentage of growth inhibition was evaluated using a MTT (Sigma) assay for the measurement of viable cells. A total of 4×10^3 cells/well was seeded onto a 96-well plate for 24 h, treated with various concentrations of the tested peptides, then incubated for an additional 24 h at 37 ^{o}C. Subsequently, 10 µl of MTT at a concentration of 5 mg/ml was added to each of the wells, and the cells were incubated for an additional 4 h. The supernatants were aspirated and 100 µl of DMSO were added to the wells in order to dissolve any remaining precipitate. Absorbance was then measured at a wavelength of 570 nm using an EL_X800 reader (Bio-Tek instruments, Inc., Winooski, VT).

2.2.6. Bactericidal assay

The kinetics of bacterial killing by the peptides was evaluated using *E. coli* CCARM 1229 and *S. aureus* CCARM 3090. Mid-logarithmic growth phase bacteria (2 x 10^5 CFU/ml) were incubated with 1X and 2X MIC peptides at 37 °C. Aliquots were removed at indicated times, appropriately diluted, plated on LB agar plate, and then the CFU were counted after 16 h incubation at 37 °C.

2.2.7. Fungicidal assay

The activities of the peptides against the *C. albicans* were tested by using standard microdilution plate candidacidal assays [60]. Midlogarithmic growth phase of *C. albicans* were grown in YPD medium and then washed with PBS. The *C. albicans* cells (2x 10^4 spore/ml) were mixed with MIC concentration of the peptides and incubated at 28 °C, aliquots were removed at fixed time internals, appropriately diluted,

plated on YPD agar plate, and then the CFU were counted after 16-24 h incubation at 28 °C.

To determine whether the candidacidal activity of these peptides is dependent on the metabolic of candida, a killing assay was performed as described above with peptides in the presence of 5 mM sodimu azide, which blocks mitochondrial respiration [61]. In this experiment, cells were incubated with sodium azide (5 mM) for 30 min at 28 °C, prior to the addition of the peptides. The optimal concentration of sodim azide (5 mM) was determined in preliminary experiments to avoid toxic effects of this compound on *C. albicans.*

2.2.8. Aggregation in aqueous solution

I compared the aggregation state of the peptides in water and in PBS by examining the fluorescence of tryptophan as a function of the peptide concentration, from 1 to 18 µM. The changes in emissions were recorded using a spectrofluorometer (Perkin-Elmer LS55, Mid Glamorgan, UK) at an excitation wavelength of 280 nm and an emission wavelength of 300 to 400 nm.

CD spectroscopy was used to determine the aggregation state of the peptides in PBS, at various concentrations in the range of 25 to150 µM.

Thioflavin T (ThT) assay was also used to determine the aggregation state of the peptides. Briefly, various concentration of peptide was mixed with 20 µM of ThT in appropriate medium in a final volume of 200 µl. The flourescence emission was recorded at room temperature using 440 nm excitation and 490 nm emissions on microplate spectrofluorometer gemini-XS (Molecular Devices CA, USA).

2.2.9. Dansyl polymyxin B displacement assay

The binding affinity of each peptide for LPS was determined by using the dansyl polymyxin B (PMB) displacement assay [62]. Dansyl PMB (4 μM/ml) and *P. aeruginosa* (9 μg/ml) were mixed in 1 ml of 5 mM HEPES (pH, 7.2), resulting in maximum fluorescence. The decrease in fluorescence was used to calculate the percent displacement of dansyl PMB due to peptide treatment. Buffer blank was subtracted from ppetide spectra. Spectra were recorded on a Perkin-Elmer LS-50B spectrofluorimeter using a cuvette with a path length of 1 cm. The excitation and emission wavelengths were 340 and 350-600 nm, respectively.

2.2.10. Binding assay with fungal cell wall components

Assay for binding of $(KW)_4$ to the surface of *C. albicans* was examined by assessing the effect of fungal cell wall components on the anti-candida activity of $(KW)_4$ was examined by microplate plate candidacidal assay [63] and ultrasensitive radial diffusion assay [64]. The MIC concentration of peptide was incubated with different concentration of cell wall components (0.5-8 mg/ml) for 1 hr at 37 ^{o}C. The effect of polysaccharide on killing of $(KW)_4$ was assessed by microdilution plate candidacidal assay descibed above.

For radial diffusion assay, $(KW)_4$ (20 μl) (final concentration = 8 μM) was added to 80 μl of each polysaccharide (0.5-8 mg ml^{-1} in PBS, pH 7.2) including laminarin (Beta-1,3-glucan polymer; sigma), or mannan (mannose polymer; sigma) and incubated with *C. albicans* cells for 1 h at 37 ^{o}C. Eight microliters sample were loaded into 3 mm diameter wells that have been punched in underlay gels in which the wahsed yeast-phase *C. albicans* (2 X 10^4 spore/ml) were trapped. The underlay agars consisted of PBS, 1% w/v agarose (sigma), and 0.3mg of YPD/ml. After incubation at 37 ^{o}C for 3 h, a 10 ml of overlay gel of 1% agarose and 6% YPD poured on the underlay gel. After the plate were incubated overnight at 37 ^{o}C to allow surviving *C. albicans* cells to form

colonies, the diameters of clearing zones indicating antifungal activity were plotted agaisnt polysaccharide concentrations. Experiments were performed in triplicate, and mean values were used to make a graph.

Next, the secondary structure was monitored at a concentration of 50 μM of $(KW)_4$ in buffer, in the presence of laminarin from digitata laminarin (0.05%; sigma-aldrich, St. Luis, USA), and in the presence of mannan from saccharomyces cerevisiae (0.05%; sigma-aldrich, St. Luis, USA).

2.2.11. Confocal laser scanning microscopy (CLSM)

To determine the cellualr distribution of $(KW)_4$, *E. coli* CCARM 1229, *S. aureus* CCARM 3090 and *C. albicans* incubated with TAMRA-labeled $(KW)_4$ were observed on a CLSM. After incubation for 10 min, the cells were pelleted by centrifugation at 3000 rpm for 5 min and washed three times with ice-cold PBS. The action site of TAMRA-labeled $(KW)_4$ was examined using an inverted LSM510 laser-scanning microscope (Carl Zeiss, Göttingen, Germany). To simultaneously detect intracellular TAMRA-$(KW)_4$, the 405 nm light from a diode laser and 543-nm light from a helium neon laser were directed at a UV/543 beam splitter. Images were then recorded digitally in a 512 x 512 pixel format.

2.2.12. Membrane depolarization

The membrane-depolarizing activity of the peptides was measured with Gram-positive bacteria, Gram-negative bacteria and fungai using the same experimental conditions performed previously [65,66]. *E. coli* CCARM 1229 and *S. aureus* CCARM 3090 were grown to mid-logarithmic phase at 37 °C with gentle agitation. *C. albicans* was grown to mid-logarithmic phase at 28 °C with gentle agitation. The cells were washed twice in buffer (20 mM glucose, 5 mM HEPES, PH 7.3) and re-suspended to an OD_{600} of 0.05 in a similar buffer, containing 0.1 M KCl. The cells were then incubated

with 1 μM $DiSC_3$-5 until stable baseline fluorescence was achieved. After addition of peptide at indicated concentrations, the change in fluorescence was measured with excitation wavelength of 622 nm and emission wavelength of 670 nm. The fluorescence of the cells with Triton X-100 (0.1%) gave to maximum depolarization.

2.2.13. SYTOX Green uptake

Membrane permeabilization of microbial cells was determined using the fluorescent dye SYTOX Green [67]. Pre-cultured cells were re-suspended (2 x 10^7 CFU/ml) in PBS and were incubated with 1 μM SYTOX Green (Molecular probes, Eugene, OR) for 10 min in the dark, peptides were added to the cell suspension, and the increase of fluorescence was measured with excitation wavelength at 485 nm and emission at 520 nm for 60 min.

2.2.14. PI uptake based fluorescence microscopic analysis of cell permeabilization by peptides.

Cell permeability was monitored using the DNA-staining fluorescent probe propidium iodide (PI) as previously described [68]. *C. albicans* cells were grown overnight in YPD media. Cells were harvested by centrifugation (4000 rpm for 10 min), washed, and resuspended in PBS to yield 2 x 10^4 spore/ml; 100 μl of *C. albicans* suspensions (2 x 10^4 spore/ml) were incubated with 5 μl from respective peptide aqueous stock solutions to yield a final peptide concentration of 8 μM ($(KW)_4$), 4 μM (melittin) for 30 min at 28°C. PI was added to each sample at a final concentration of 1 μM and the plate was incubated at 28 °C for 5 min. The effects of peptides against *C. albicans* were visualized by an inverted fluorescence phase contrast microscope (IX71, Olympus, Tokyo, Japan) under PI filters. Cells without peptide served as a control.

2.2.15. Preparation of small and large unilamellar vesicles (SUVs and LUVs)

SUVs were prepared by sonication method with required amount of either PE:PG (7:3, w/w) or PC:CH (10:1, w/w) or PE:PC:PI:ergosterol (5:4:1:2, w/w/w/w) or PC:CH:SM (1:1:1, w/w/w). Dry lipids were dissolved with chloroform in a glass vessel. Solvents were removed over a stream of nitrogen gas and then lyophilized overnight to remove trace amount of organic solvent. The dry lipid film was resuspended in PBS at pH 7.2 with gentle vortex mixing. The lipid suspensions were then sonicated at 40 °C with bath-type ultrasonicator until the solution became clear. The lipid suspension was extruded fourteen times through polycarbonate filters with 0.05 μm pore size using an Avanti Mini-Extruder (Avanti Polar Lipids Inc., Alabaster, AL).

Large unilamellar vesicles (LUVs) were prepared by freeze-thaw method [69, 70]. Dry lipid films were resuspended in 1-2 ml of appropriate buffer by vortexing. LUVs were prepared by nine freeze-thaw cycles under liquid nitrogen and water bath at 50 °C. After preparation of vesicles, suspensions were then extruded fourteen times through a 0.2 μm pore polycarbonate membrane. Lipid concentration was determined by a standard phosphate assay [71].

2.2.16. Calcein leakage from liposomes

Permeabilization of liposomes by the peptides was assayed by meauring leakage of entrapped calcein. Calcein-entrapped LUVs composed of PE:PG (7:3, w/w) or PC:CH (10:1, w/w) or PE:PC:PI:ergosterol (5:4:1:2, w/w) or PC:CH:SM (1:1:1, w/w) were prepared by vortexing the dried lipid in a dye buffer solution (70 mM calcein, PBS, pH 7.4). The suspension was freeze-thawed in liquid nitrogen for nine cycles and then the calcein-entrapped vesicles were separated from free calcein by gel

filtration chromatography on a Sephadex G-50 column. Entrapped LUVs in a suspension containing 2.5 μM lipids were then incubated with various concentrations of the peptide (0.03-1 μM) for 25 min. The fluorescence of the released calcein was assessed using a spectrofluorometer at an excitation wavelength of 480 nm and an emission wavelength of 520 nm. Complete (100%) release was achieved via the addition of 0.1% Triton X-100. Spontaneous leakage was determined to be negligible. All experiments were conducted at 25 ^{o}C and the apparent percentage of calcein that was release was calculated according to the following equation [72]:

$$\text{Release (\%)} = 100 \times (F - F_o)/(F_t - F_o)$$

in which F and F_t represent the fluorescence intensity prior to and after the addition of the detergent, respectively, and F_o represents the fluorescence of the intact vesicles.

2.2.17. Liposome aggregation

Aggregation of lipid vesicles was monitored by visible absorbance measurements. The buffer used was PBS, pH 7.2. Peptides (5, 10, 20 and 40 μM) in PBS solutions were added to a suspension of 400 μM LUVs consisting of PE:PG (7:3, w/w) or PC:CH:SM (1:1:1, w/w). Increase of absorbance indicates the aggregation of liposomes. Absorbance was measures at 405 nm using a microplate Autoreader before and after the addition of peptide [73,74].

2.2.18. Tryptophan fluorescence and acrylamide quenching assay

The fluorescence emission spectrum of Trp of peptides was monitored in the presence of PE:PG (7:3, w/w) or PC:CH (10:1, w/w) or PE:PC:PI:ergosterol (5:4:1:2, w/w/w/w) or PC:CH:SM (1:1:1, w/w) SUVs. In these fluorescence studies, SUVs were used to minimize differential light scattering effects [75]. The Trp fluorescence measurements were taken with spectrofluorometer. Each peptide was added to 1 ml of 200 μM liposomes, and the peptide:liposome mixture (a molar ratio of 1:100) was

allowed to interact at 25 °C for 10 min. The fluorescence was excited at 280 nm, and the emission was scanned from 300 to 400 nm.

For fluorescence quenching experiments were conducted using acrylamide as the quencher. The acrylamide concentration in the cuvette was between 0.04 to 0.20 M. The effect of acrylamide on the fluorescence of each peptide was analyzed with a Stern-Volmer equation:

$$F_0/F=1+K_{SV}\,(Q)$$

Where F_0 and F represent the fluorescence intensities in the absence and the presence of acrylamide, respectively, K_{SV} is the Stern-Volmer quenching constant, and (Q) is the concentration of acrylamide.

2.2.19. Circular dichroism (CD) spectroscopy

The CD spectra were recorded on a Jasco 810 spectropolarimeter (Jasco, Tokyo, Japan) which was equipped with a temperature control unit, using a 0.1-cm path-length quartz cell at 25 ^{o}C between 190 and 250 nm. The CD spectra were measured for peptide samples (50 μM) that were dissolved in PBS alone (pH 7.2) and PBS containing 1 mM PE:PG (7:3, w/w) or PBS containing 1 mM PC:CH (10:1, w/w) or PBS containing PE:PC:PI:ergosterol (5:4:1:2, w/w/w/w) or PBS containing PC:CH:SM (1:1:1, w/w) SUVs vesicles. The peptides (50 μM) were scanned in the presence or absence of LPS (0.1%) dissolved in PBS. CD data represent average value from three separate recordings, with four scans per sample.

2.2.20. Scanning electron microscopy (SEM)

A mid-logarithmic phase culture of *E. coli* CCARM 1229 or *C. albicans* KCTC 7270 cells were re-suspended at 2 x 10^7 CFU/ml in PBS (pH 7.2) and incubated at 37 °C and 28°C respectively, with $(KW)_4$ at MIC concentration. A control was run in the absence of peptide solution. After 60 min, the bacteria cells were pelleted by

centrifugation at 3000xg for 5 min and washed twice in PBS. The supernatants were removed and the pellets were fixed in 500 µl of 5% (v/v) glutaraldehyde in 0.2 M sodium-cacodylate buffer (pH 7.4). After fixation for 3 h at 4 °C, the samples were extensively washed with 0.1 M sodium-cacodylate buffer. The samples were then treated with 1% (w/v) osmium tetroxide in 0.1 M sodium-cacodylate buffer, in the dark for 1 h at 4 °C. The bacteria cells were then washed twice in 5% (w/v) sucrose in same buffer and then dehydrated in 20, 40, 60, 80, 95 and 100% ethanol, sequentially. After lyophilization and good coating, the samples were examined using a scanning electron microscope (Hitachi S-2400N, Japan).

3. Results

3.1. Influences of a repetitive pattern of lysine and tryptophan on antibacterial activity and mechanism of action

(1) Effects of hydrophobicity and length of $(KW)_n$ peptides on antibacterial and hemolytic activities

Reversed phase-HPLC was used to determine the peptide hydrophobicity and to elucidate its influence on antibacterial and hemolytic activity. Table 1 shows that the increase in retention time and relative hydrophobicity of the $(KW)_n$ peptides, which followed the order $(KW)_2 < (KW)_3 < (KW)_4 < (KW)_5$, reflecting changes in the total hydrophobicity as the addition of amino acids (K/W).

Their antibacterial activities were listed in Table 1, the $(KW)_2$ peptide was inactive against all strains, but $(KW)_3$ showed improved activity against *S. typhimurium*, *P. aeruginosa* and *L. monocytogenes*. $(KW)_4$ peptide displayed a potent antibacterial activity with a broad-spectrum. Interestingly, $(KW)_5$ peptide retained a similar activity to $(KW)_4$ in the presence of PBS. In low ionic strength buffer (sodium phosphate (SP) buffer), $(KW)_4$ peptide showed more potent activity than all other studied peptides against all strains.

The hemolytic activity of peptides was measured using hRBCs. The $(KW)_2$ and $(KW)_3$ peptides were non-hemolytic, but $(KW)_4$ and $(KW)_5$ peptides caused 8% and 71% hemolysis at 200 μM, respectively (Table 1). $(KW)_5$ was hemolytic because they have higher hydrophobicity than the others.

Table 1. MICs of the peptides against bacterial strains

	MIC (μM)						
Microorgaisms	$(KW)_2$	$(KW)_3$	$(KW)_4$	$(KW)_5$	Melittin	Ampicillin	Oxacillin
Gram (-) bacteria							
E. coli	>200 (>200)	50 (200)	6.25 (12.5)	50 (12.5)	1.56 (1.56)	50	-
S. typhimurium	50 (200)	3.12 (6.25)	1.56 (1.56)	6.25 (3.12)	0.39 (0.39)	25	-
P. aeruginosa	>200 (>200)	12.5 (25)	3.12 (3.12)	25 (6.25)	3.12 (3.12)	-	-
Gram (+) bacteria							-
S. aureus	>200 (>200)	50 (200)	6.25 (12.5)	25 (12.5)	1.56 (1.56)	-	12.5
B. subtilis	>200 (>200)	100 (200)	6.25 (12.5)	12.5 (12.5)	1.56 (3.12)	-	-
L. monocytogenes	200 (>200)	12.5 (25)	3.12 (3.12)	3.12 (3.12)	1.56 (1.56)	-	-
Resistant strains							
E. coli CCARM 1229[a]	>200 (>200)	25 (100)	6.25 (12.5)	50 (12.5)	3.12 (3.12)	>200 (>200)	
E. coli CCARM 1238[a]	>200 (>200)	50 (200)	12.5 (12.5)	50 (12.5)	1.56 (1.56)	>200 (>200)	
S.typhimurium CCARM 8007[b]	>200 (>200)	50 (200)	12.5 (12.5)	25 (12.5)	6.25 (12.5)	>200 (>200)	
S. typhimurium CCARM 8009[b]	>200 (>200)	50 (200)	6.25 (12.5)	25 (12.5)	6.25 (12.5)	>200 (>200)	
S. typhimurium CCARM 8013[b]	>200 (>200)	50 (200)	6.25 (12.5)	25 (12.5)	3.12 (6.25)	>200 (>200)	
S. aureus CCARM 3089[c]	>200 (>200)	50 (200)	12.5 (12.5)	50 (12.5)	1.56 (1.56)	-	>200 (>200)
S. aureus CCARM 3090[c]	>200 (>200)	50 (200)	12.5 (12.5)	25 (12.5)	3.12 (3.12)	-	>200 (>200)
S. aureus CCARM 3108[c]	>200 (>200)	50 (200)	12.5 (12.5)	50 (12.5)	1.56 (1.56)	-	>200 (>200)
S. aureus CCARM 3114[c]	>200 (>200)	50 (200)	12.5 (12.5)	25 (12.5)	3.12 (3.12)	-	>200 (>200)
S. aureus CCARM 3126[c]	>200 (>200)	50 (200)	12.5 (12.5)	25 (12.5)	1.56 (1.56)	-	>200 (>200)
Hemolysis[d] (%)	0	0	8	71	100	-	-
Retention time[e]	17.6	19.5	21.7	23.8	-	-	-
Relative hydrophobicity[f] (cationicity)[g]	28 (+3)[g]	31 (+4)[g]	34 (+5)[g]	38 (+6)[g]	-	-	-

Antibacterial assay was performed in 10 mM sodium phosphate buffer, pH 7.2 and phosphate buffered saline, pH 7.2 (number in the parenthesis)

[a]Drug-resistant *Escherichia coli* strains.

[b]Drug-resistant *Salmonella typhimurium* strains.

[c]Drug-resistant *Staphylococcus aureus* strains.

[d]Hemolytic percentage at 200 μM of peptide in phosphate buffered saline

[e]Retention time was measured by using a C_{18} reverse phase analytical column (4.6 x 250 mm, 300 Å, 5 nm). The peptides were eluted over 60 min, using a linear gradient of 5% to acetonitrile in water containing 0.05% (v/v) trifluoroacetic acid.

[f]relative hydrophobicity is reflected by the percent of acetonitrile at the retention time [76].

[g]Cationicity (number in the parenthesis)

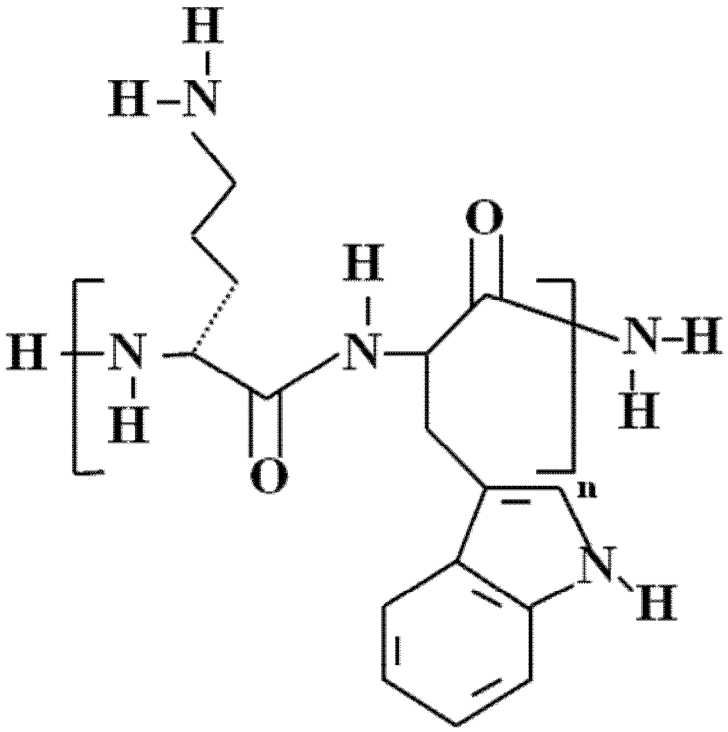

Figure 1. Chemical structure of linear antimicrobial peptides, $(KW)_n$ $–NH_2$, used in this study, where n=2,3,4 and 5

(2) Structure and organization of $(KW)_n$ peptides in aqueous solution

In order to ascertain a relationship between the aggregation states in aqueous solution and activities of the peptides, self aggregation of $(KW)_4$ or $(KW)_5$ was examined in water and PBS. Both peptides did not aggregate in water, being indicated by Trp fluorescence (Fig. 2A). The emission maximum of Trp fluorescence in $(KW)_5$ peptide was dose-dependently shifted from 352 to 340 nm in PBS (Fig. 2B), indicating to self aggregation of $(KW)_5$, whereas, that of $(KW)_4$ peptide was not changed, which means to be soluble.

The aggregation states of above peptides were further analyzed using CD spectroscopy. In PBS (Fig. 2C-D), Trp-containing peptides show a negative band at 200 nm region. This band is characteristic of a random coil, while the band at 225 nm is related to the Trp side chain in $(KW)_n$ which contributed to the CD signal in this spectral region [33,77,78]. The CD spectra of $(KW)_5$ was random coil, indicating that they had failed formation into the β-sheet conformation at concentrations of 25, 50 μM. At higher concentration of 100, 150 μM, the negative band moved to higher wavelength, indicating that a very small ratio of $(KW)_5$ probably adopted β-sheet (Fig. 2D). This conformation likely implies that the $(KW)_5$ peptide might adopt weakly or small aggregates, but the $(KW)_4$ peptide maintain its complete soluble form in PBS.

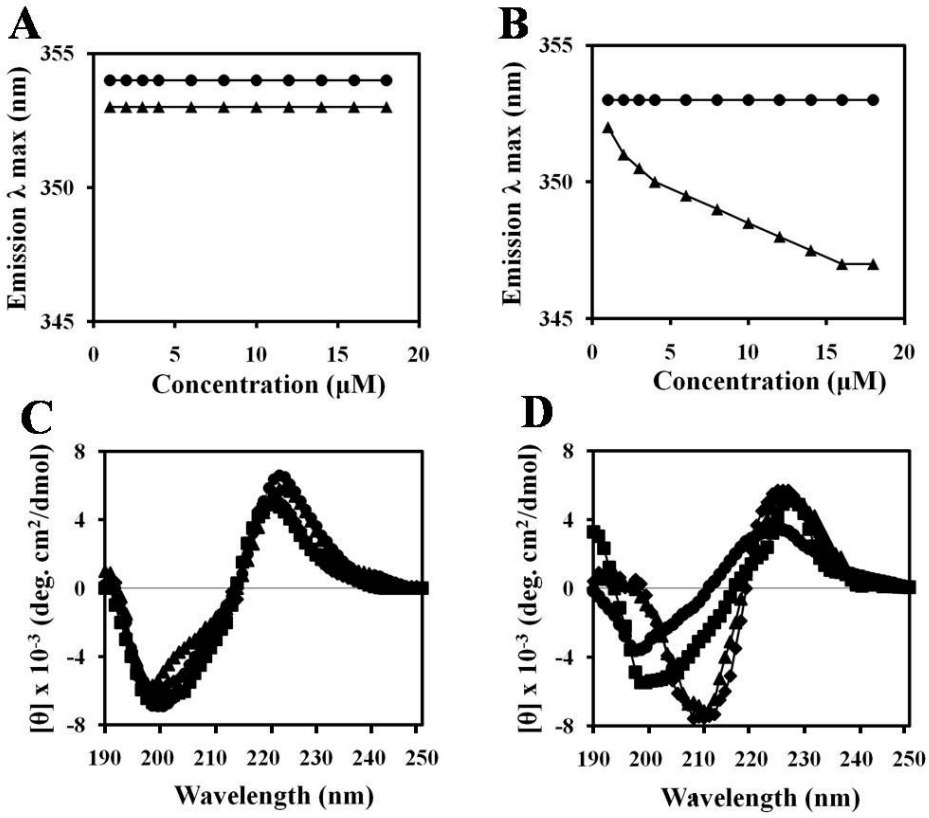

Figure 2. Structure and organization of $(KW)_4$ and $(KW)_5$ peptides in aqueous solution. Aggregation state of peptides in aqueous solution was determined using the fluorescence of Trp as a function of peptide concentrations. The wavelength at maximum emission was taken for plotting. $(KW)_4$ (●), $(KW)_5$ (▲) : Water (A) and PBS, pH 7.2 (B). Concentrations dependent CD spectroscopy was used to examine the conformation of the soluble or aggregation state of these peptides. Concentrations dependent CD spectra of $(KW)_4$ (C) and $(KW)_5$ (D) in PBS, pH 7.2: 25 μM (●), 50 μM (■), 100 μM (▲), 150 μM (♦).

(3) Localization of fluorescence-labeled peptides

In order to a examine the target site of $(KW)_4$ peptide on *E. coli* CCARM 1229 and *S. aureus* CCARM 3090, bacteria was treated with the peptide and observed under CLSM. Results showed that peptides bound with the cell surface of bacteria (Fig. 3), indicating interaction with the bacterial membrane surface.

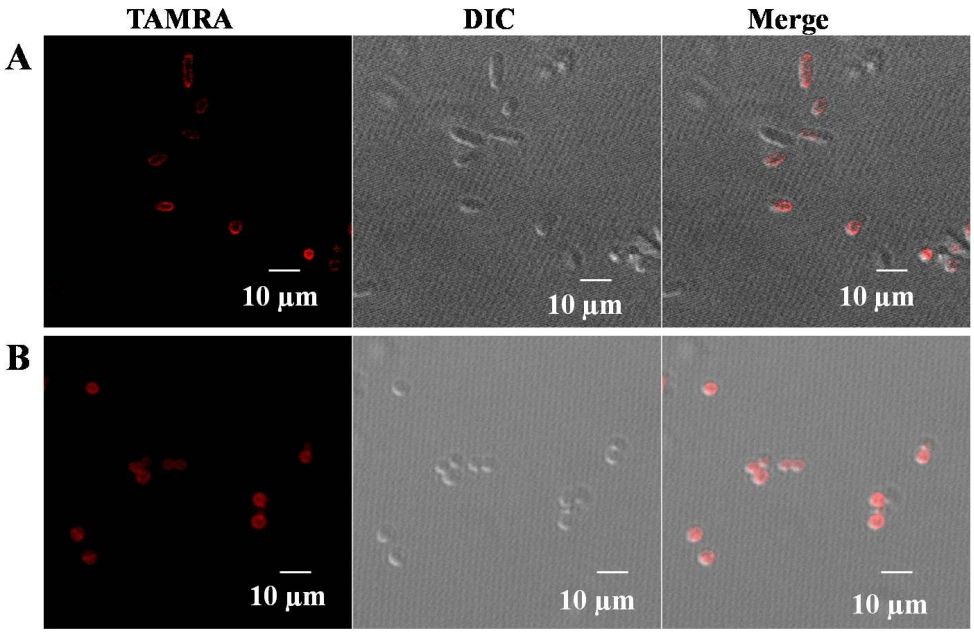

Figure 3. Confocal laser scanning microscopy images of *E. coli* CCARM 1229 (A) and *S. aureus* CCARM 3090 (B) cells treated with TAMRA-labeled-$(KW)_4$. The cells were treated with 12.5 µM of TAMRA-$(KW)_4$ for 10 minutes at 37 °C in PBS, pH 7.2. From left to right: TAMRA, differential interference contrast (DIC), and merged images.

(4) The interaction of peptides with LPS

As shown in Figure 4A, the LPS-binding affinity of $(KW)_n$ peptide was increased in chain-length dependent manner. The 20 μM of $(KW)_5$ peptide with the highest LPS-binding affinity resulted in 81% maximal displacement of dansyl PMB from LPS, whereas $(KW)_4$, $(KW)_3$, or $(KW)_2$ was measured to 60, 55, or 40% binding affinity, respectivelly.

Next CD predicted interaction of the peptides (at 50 μM) in LPS (0.1%) (Fig. 4B). The $(KW)_2$ and $(KW)_3$ did not give any secondary structures, while the longer peptides adapted β-sheet conformation, indicating that the longer peptides strongly bind to LPS, which is highly correlated with their displacemrnt of dansyl PMB.

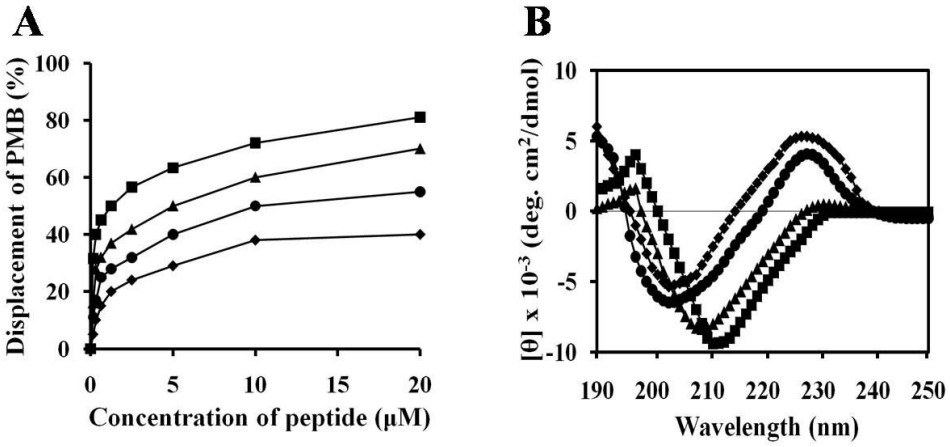

Figure 4. Binding affinities of the peptides for LPS as measured by the dansyl polymyxin B (DPX) displacement assay. *P. aeruginosa* LPS (9 µg) was incubated with dansyl polymyxin B (4 µM) for 5 min, and the fluorescence was measured at an excitation of 340 nm and emission of 485 nm. Peptides was added in different concentrations and the DPX fluorescence was meaured after 5 min. $(KW)_2$ (♦), $(KW)_3$ (●), $(KW)_4$ (▲), $(KW)_5$ (■). CD spectra of the peptides (50 µM) were measured in the presence of 0.1% LPS (B): $(KW)_2$ (♦), $(KW)_3$ (●), $(KW)_4$ (▲), $(KW)_5$ (■).

(5) Membranolytic and bactericidal activity

The direct disruption of scrambled peptides in the membrane potential of the cytoplasmic membrane was determined in *E. coli* and *S. aureus*. Fig. 5A and B showed the dose-dependent dissipation of the membrane potential by peptides against intact cells of *E. coli* CCARM 1229 (Fig. 5A) and *S. aureus* CCARM 3090 (Fig. 5B). The ability of the longer peptides $(KW)_4$ or $(KW)_5$ to dissipate the bacterial membrane potential, correlates with their antibacterial activity against *E. coli* and *S. aureus* (Table 1). In contrast, inactive $(KW)_2$ did not depolarize the membrane and $(KW)_3$ peptide which has the lowest antibacterial activity, also had a depolarizing activity less than longer peptides.

The uptakes of the fluorescent dye, SYTOX Green were accessed to determine the membrane permeability of these peptides against *E. coli* and *S. aureus*. The influx of SYTOX Green fluorescence was measured for 60 min after the addition of 12.5 μM peptide in PBS. The $(KW)_4$ and $(KW)_5$ peptides showed a significant dye uptake within 35 min in *E. coli* (Fig. 5C) and *S. aureus* cells (Fig. 5D). The $(KW)_3$ peptide caused less uptake than them, while inactive $(KW)_2$ peptide had no permeabilization effect on the bacterial membrane. These results indicate that longer peptides exert a potent antibacterial action through membrane-disrupting action

The bactericidal action of $(KW)_4$ and $(KW)_5$ peptides were investigated using the time-killing assay. Fig. 5E and F were shown the time-killing studies of the peptides against both *E. coli* CCARM 1229 (Fig. 5E) and *S. aureus* CCARM 3090 (Fig. 5F): at concentration equal to or above the MIC, bacterial counts with both peptides were significantly decreased within 35 min. The $(KW)_5$ peptide killed bacteria more quickly than $(KW)_4$ due to the effect of chain length or hydrophobicity, being consistent with their faster membrane permeability on the bacterial membrane (Fig. 5C-D).

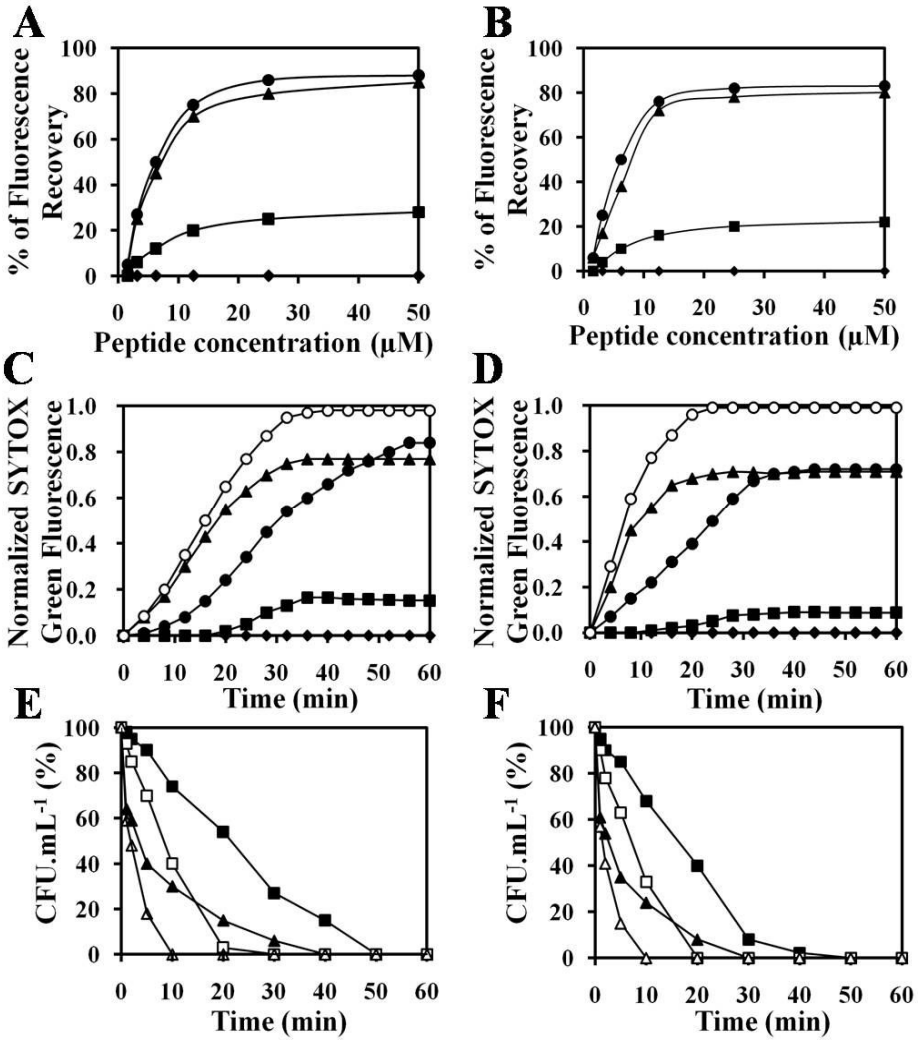

Figure 5. Membrane disrupting and bactericidal activity. Dose-response curves of the membrane depolarization activities of the peptides against intact *E. coli* CCARM 1229 (A) and *S. aureus* CCARM 3090 (B). Membrane depolarization was monitored by an increase in the fluorescence of $DiSC_3$-5 (excitation wavelength λex = 620 nm; emission wavelength λem = 670 nm) after the addition of peptide at different concentrations: $(KW)_2$ (♦), $(KW)_3$ (■), $(KW)_4$ (●), $(KW)_5$ (▲). The fluorescence increase obtained

using 0.1% Triton X-100 was taken as 100%. Membrane permeabilization was monitored by entry of SYTOX Green dye. Bacteria cells (2 x 10^7 CFU/ml) in PBS were incubated with 1 μM SYTOX Green dye. Peptides were added at 12.5 μM concentration and the uptake of the dye through the plasma membrane was measured by the time course of fluorescence at an excitation at 485 nm and emission at 520 nm which shows the uptake of SYTOX Green in *E. coli* (C) and *S. aureus* (D): $(KW)_2$ (♦), $(KW)_3$ (■), $(KW)_4$ (●), $(KW)_5$ (▲), and Melittin (○). Kinetics of the bactericidal activity of the peptides against *E. coli* CCARM 1229 (E) and *S. aureus* CCARM 3090 (F). Bacteria treated with the respective peptides were diluted at the appropriate times and then plated on LB agar. The CFU were then counted after 16 h of incubation at 37 °C. Black, $(KW)_4$; White, $(KW)_5$; squares and triangles 1 and 2 times the MIC value, respectively; cells (2 x 10^5 CFU/ml) incubated in the absence of any peptide served as controls

(6) Calcein release from liposomes and turbidity assay

A calcein leakage assay was used to investigate interactions between AMPs and artificial membranes. PE:PG (7:3, w/w) vesicles with $(KW)_4$ at 2.5:1 lipid-to-peptide molar ratio (L/P) displayed a maximum leakage of 81%, while the $(KW)_5$ did 73% of leakage. The $(KW)_3$ showed to be moderate active, but $(KW)_2$ are inactive in this assay (Fig. 6A). In zwitterionic liposomes of PC:CH (10:1, w/w), $(KW)_5$ and $(KW)_4$ peptides were released 80% and 30% calceins at 2.5:1 L/P ratio, respectively (Fig. 6B). These results were consistent with their hemolytic activities, as shown in Table 1. The small peptides $(KW)_2$ and $(KW)_3$ showed no leakage from zwitterionic membrane.

To investigate peptide's action in the membrane, the turbidity of PE:PG vesicles was measured after the adding of peptides. Peptides induced the dose-dependent increases of absorbance (Fig. 6C), indicating to aggregation of vesicles via membranolytic action of peptides. The results indicate that the size of the vesicle was increased due to lysis and aggregation.

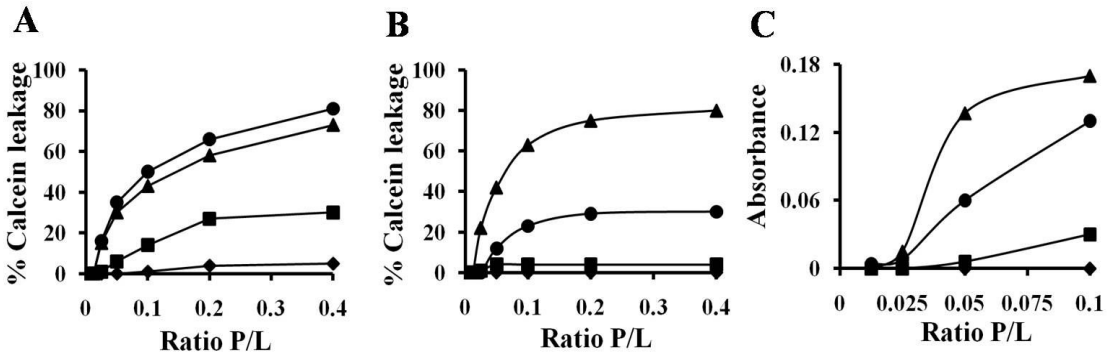

Figure 6. The action of peptides on artifical liposomes. Dose dependent percent leakage of calcein from PE:PG (7:3, w/w) (A) and PC:CH (10:1, w/w) (B) at pH 7.4 was measured for 15 min after the addition of the peptide. LUV aggregation as a function of peptide concentration (C). Peptide solutions were added to a suspension of 400 μM LUVs consisting of PE:PG (7:3, w/w) and aggregation was monitored by absorbance change of LUVs at 405 nm: $(KW)_2$ (♦), $(KW)_3$ (■), $(KW)_4$ (●), $(KW)_5$ (▲).

(7) Characterization of the tryptophan environment using fluorescence spectroscopy

Peptide binding into lipid bilayers was examined by recording the Trp fluorescence emission spectra in PBS and in the presence of vesicles composed of negatively charged PE:PG (7:3, w/w) or zwitterionic PC:CH (10:1, w/w). The data in Table 2 suggest that the fluorescence spectra of $(KW)_n$ peptides in buffer gave rise to a maximum fluorescence peak at around 353 nm except for $(KW)_5$, indicating that the Trp residue of these peptide are located in a more hydrophilic environment. But, Trp residues of $(KW)_5$ move from a polar to less polar environment, may be due to their self aggregation ability in PBS (Fig. 2). In PE:PG (7:3, w/w) vesicles, the order of membrane binding ability of these peptides is $(KW)_4 > (KW)_5 > (KW)_3 > (KW)_2$. Among them, larger blue shift of $(KW)_4$ peptide suggested that the Trp side chain partitions preferentially into a more rigid, hydrophobic environment in PE:PG (7:3, w/w) lipid bilayers. In the presence of PC:CH (10:1, w/w) vesicles, a blue shift in the Trp emission of $(KW)_5$ (342 nm) was observed, reflecting their location to more hydrophobic environments [79]. On the other hand, the blue shift of $(KW)_2$, $(KW)_3$ and $(KW)_4$ were not observed in more hydrophobic environment.

The accessibility of Trp residues into lipid bilayers can be determined by measuring the stern-volmer quenching constants for each peptide, using soluble acrylamide as a quencher. The free Trp residues in aqueous solution was fully quenched by acrylamide, having a stern-volmer quenching constant (K_{SV}) of about 9 M^{-1} [80]. The data showed to the K_{SV} value of about 15, 15, 14, 11 M^{-1} for the $(KW)_2$, $(KW)_3$, $(KW)_4$ and $(KW)_5$ peptides in PBS, respectively (Table 2). K_{SV} for the $(KW)_4$ peptide is 1.6 M^{-1}, indicating that the Trp residues of $(KW)_4$ are more protected in the presence of PE:PG (7:3, w/w) vesicles than in PC:CH (10:1, w/w) (Table 2). This

tendency is consistent with the potent antibacterial activity of $(KW)_4$. The hemolytic peptide, $(KW)_5$ had a lower K_{SV} value, suggesting that its Trp residues of $(KW)_5$ peptide is more anchored within the hydrophobic core of the zwitterionic phospholipids, which is likely correlates strong effect at inducing calcein leakage from the same synthetic membrane (Fig. 6B).

Table 2. Tryptophan emission maxima of 2 μM peptides and *K*sv in PBS (pH 7.2) or in the presence of 200 μM PE:PG (7:3, w/w) SUVs and 200 μM PC:CH (10:1, w/w) SUVs

Peptides	λ_{max} buffer (nm)	Blue shift (nm)		*K*sv (M^{-1})[a]		
		PE:PG (7:3, w/w)	PC:CH (10:1, w/w)	Buffer	PE:PG (7:3, w/w)	PC:CH (10:1, w/w)
$(KW)_2$	353	8	2	15	2.8	5.8
$(KW)_3$	353	11	2	15	2.3	5.3
$(KW)_4$	353	17	5	14	1.6	5.1
$(KW)_5$	351	14	9	11	2.0	4.3

[a]K_{SV} is the Stern-Volmer constants. K_{SV} (M^{-1}) were determined from the Stern Volmer equation $F_0/F_1 = 1 + K_{SV}$ (Q), where Q is the concentration of quencher (acrylamide). Concentration of the quencher varied from 0.04 to 0.20 M.

(8) Structure of peptides in liposmes

The secondary structures of the peptides were determined in aqueous solution and lipid membrane (Fig. 7). The $(KW)_2$ and $(KW)_3$ did not attained any structure in both environments. Random coil spectrum of $(KW)_4$ and $(KW)_5$ in aqueous solution were observed. The $(KW)_4$ and $(KW)_5$ adopted β-sheet conformation in both liposomes.

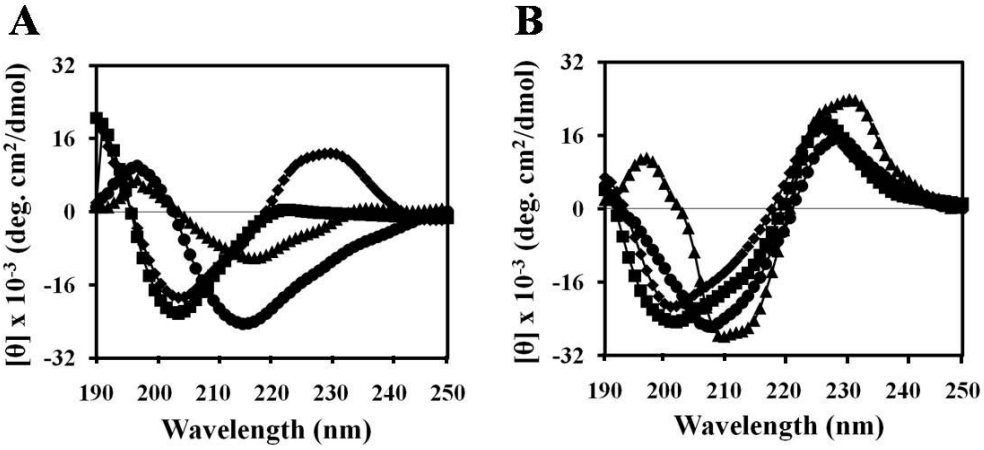

Figure 7. CD spectra of $(KW)_2$ (♦), $(KW)_3$ (■), $(KW)_4$ (●), $(KW)_5$ (▲) in the presence of PE:PG (7:3, w/w) (A) and PC:CH (10:1, w/w) (B).

(9) Observation of $(KW)_4$ peptide action in *E. coli* using scanning electron microscopy (SEM)

To investigate the action of $(KW)_4$ peptide against *E. coli* CCARM 1229, the morphological change was observed under SEM after incubation of peptide and bacterial cells. Figure 8 showed that bacteria in the absence of peptide displayed a smooth surface (Fig. 8A), in contrast, bacterial surfaces with 12.5 μM peptide were damaged and *E. coli* was aggregated (Fig. 8B).

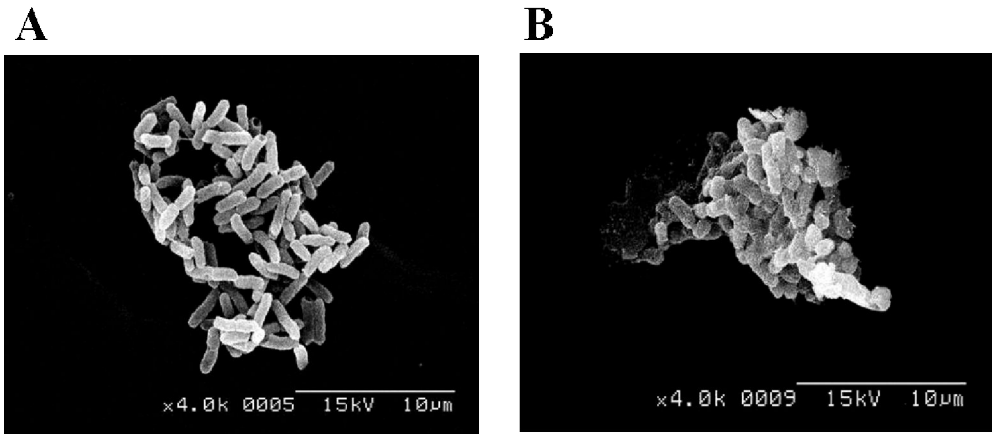

Figure 8. Scanning electron micrographs of *E. coli* CCARM 1229 cells in the absence (A) or presence (B) of $(KW)_4$ peptide (12.5 μM). The bacteria membranes were incubated with peptide for 1 h at 37 °C in PBS, pH 7.2.

3.2. Mode of action of $(KW)_n$ peptides in fungal pathogens

(1) Effects of chain length of $(KW)_n$ peptides on antifungal activity

The MIC values of these peptides against fungal strains were shown in table 3. The antifungal activity of these peptides generally increased with an increase in the chain length. The shortest peptides are inactive, but the $(KW)_3$, $(KW)_4$, and $(KW)_5$ peptides are potent antifungal activity, with MICs in the micromolar range. Interestingly, $(KW)_4$ peptide reatined a similar activity to $(KW)_5$ against *C. albicans, C. catenulate, C. rugosa* and *C. melibiosica* strains. Against resistant strain and hyphal form of *C. albicans*, $(KW)_3$ had loses its activity, while longer chains are almost active. A twofold increase in antifungal activity againt more resistant strains was noticed in the sequence of $(KW)_5$ when compared with the $(KW)_4$ peptide. Against hyphal form of *C. albicans* was found to be similar to that of $(KW)_4$.

Table 3. MICs of the peptides against fungal strains

	MIC (µM)					
Normal strains	$(KW)_2$	$(KW)_3$	$(KW)_4$	$(KW)_5$	Melittin	Fluconazol
C. albicans	>128	32	8	8	4	16
C. catenulate	>128	16	8	8	8	-
C. intermidia	>128	32	8	4	4	-
C. rugosa	>128	32	8	8	8	-
C. glabrata	>128	32	8	4	4	-
C. melibiosica	>128	32	8	8	8	-
Resistant strains						
CCARM 14001	>128	>128	32	8	16	>128
CCARM 14007	>128	>128	32	16	8	>128
CCARM 14020	>128	>128	32	8	8	>128
Hyphal condition						
C. albicans	>128	>128	64	64	32	-

(2) Effect of salt ions and pH on antifungal activity and self-association of peptide in aqueous solution

Indeed, the peptides' antimicrobial activity was gradually decreased in high ionic strength. Therefore, the antifungal activity of these peptides was determined at increasing concentration of NaCl and $MgCl_2$ (Fig. 9A-B). Antifungal activity of $(KW)_3$ against *C. albicans* was decreased, whereas longer peptides did not reduced their activity in 150 mM NaCl and 5 mM $MgCl_2$. However, $(KW)_5$ showed increased activity in higher salt conditions suggesting that aggregated peptides in low concentration of salt were dis-aggregated**.**

The peptides activity at different pH values ranged from 5.2 to 7.2 was examined to ascertain the effect of peptide concentration (Fig. 9C). This assay is very important because culture medium is changed to acidic pH when *C. albicans* are grown. There was no change in the antifungal activity of $(KW)_3$ and $(KW)_4$ were observed by all pHs . Only $(KW)_5$ peptide activity was significantly increased in low pH buffer than under basic conditions. This is due to increased solubility of $(KW)_5$ at a acidic pH.

In order to ascertain a relationship between the aggregation state and antifungal activity of the peptide, self aggregation of $(KW)_5$ was examined in a different buffer conditions by using ThT (Fig. 9D). The enhancement of ThT fluorescence when it binds to peptide represents to aggregation state with high β-sheet content. The emission maximum of ThT fluorescence in $(KW)_5$ peptide was dose-dependently increased in NaPB (sodium phosphate buffer, pH 7.2), indicating to self aggregation of $(KW)_5$. The self aggregation of $(KW)_5$ was increased in ordered from NaPB (pH 7.2) > PBS> 150 mM NaCl> 5 mM $MgCI_2$ > NaPB (pH 5.2).

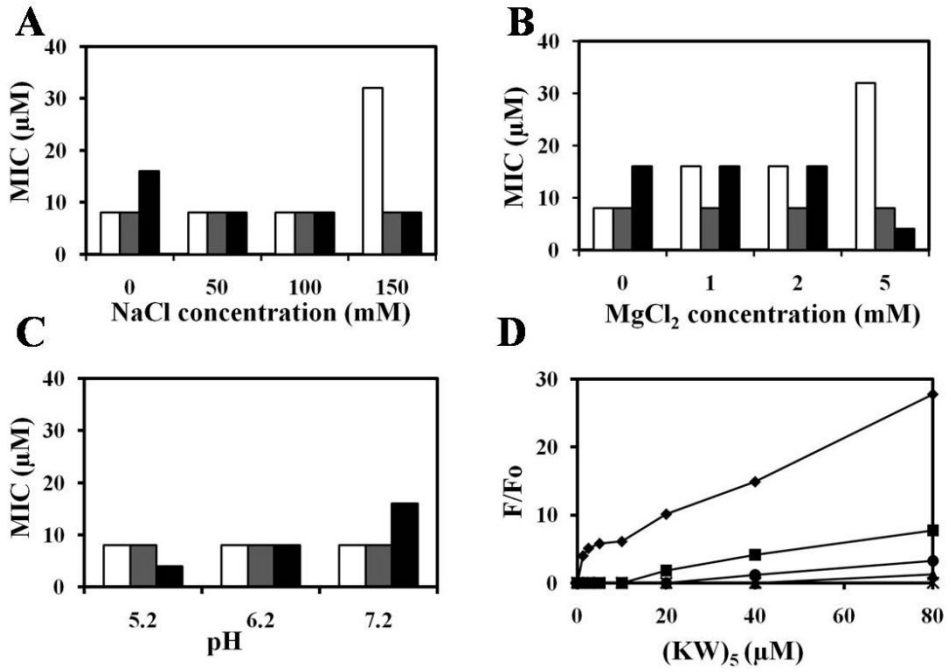

Figure 9. Effect of peptide length, salt and pH on the MICs of $(KW)_n$ peptides against *C. albicans* and self-association of peptide in aqueous solution. MICs of the peptides against *C. albicans* in the presence of 10 mm NaPB supplemented with NaCl (A), $MgCI_2$ (B). The effect of pH (C) on the antifungal activity of $(KW)_n$. $(KW)_3$ (White bars), $(KW)_4$ (Gray bars), $(KW)_5$ (Black bars). $(KW)_5$ peptide concntration effect in the ThT (20 µM) fluorescence emission intensity in different bufferd conditions or pH 5.2, with excitation at 450 nm and emission at 490 nm (F). NaPB (♦), PBS (■), 150 mM NaCl (●), 5 mM $MgCI_2$ (▲) and pH 5.2 (×).

(3) Cytototoxicity and candidacidal activity of peptide

Figure 10A shows the cytotoxicity of the peptides towards HaCaT cells. Peptide toxicity was increased linearly with their chain lengths. The $(KW)_3$ and $(KW)_4$ peptides are non-cytotoxicity, whereas the $(KW)_5$ peptide showed cytotoxicity but only above their MICs or MBCs. When comparing the lytic peptides of melittin, which induced 100% cytotoxicity at a concentration of 20 μM under similar conditions.

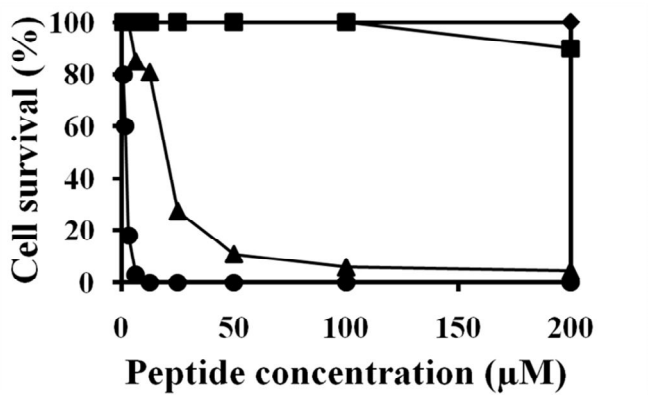

Figure 10. Cytotoxicity toward HaCaT cells. HaCaT cells (4×10^3 cell/well) were incubated for 24 h with the indicated concentrations of $(KW)_3$ (♦), $(KW)_4$ (■), $(KW)_5$ (▲) and melittin (●).

Since peptides that inhibit the growth of fungal pathogens can be either fungicidal or fungistatic, the effect of $(KW)_n$ on the viability of hyphal cells was examined (Fig. 11). I studied time-killing assay to elucidate the killing mechanism of peptide on the fungal membrane. The $(KW)_n$ peptide completely killed *C. albicans* after 3 hr at their MIC concentration. Comparative killing properties between $(KW)_n$ series against *C. albicans* showed that $(KW)_5$ was faster than $(KW)_4$ and $(KW)_3$ peptides. Furthermore, among $(KW)_n$ indicated that chain length was consistent with their faster killing activity. In the presence of 5 mM sodium azide, the fungicidal activity of these peptides was not inhibited. The same results obtained when killing was measured in the absence of 5 mM sodium azide.

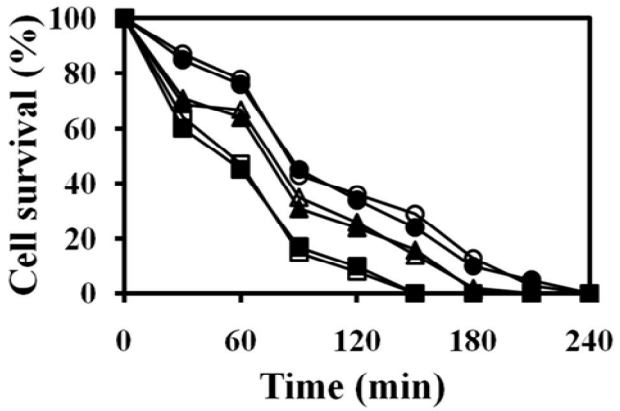

Figure 11. Time-killing kinetics of $(KW)_n$ peptides against *C. albicans* and effect of sodium azide on candidacidal activity of $(KW)_n$ peptides, determined by killing assay. *C. albicans* treated with the respective peptide were diluted at the indicated times and then plated on YPD agar. The CFU were then counted after 16-24 h of incubation at 28 ºC by counting colony forming units (CFUs). Circle (●), Triangle (▲) and square (■) represent $(KW)_3$, $(KW)_4$ and $(KW)_5$ peptides at their MIC value, respectively. Black and white represents presence of sodium azides and absence of sodium azide, respectively. Cells (2×10^4 CFU/mL) incubated in the absence of any peptide served as controls. Results represent the means of three independent experiments

(4) Interaction of peptides with fungal cell wall componenets

To determine whether these peptides have affinity with cell wall polysaccharides, this study assessed $(KW)_4$-cell wall binding and killing activity in the presence of carbohydrates major fungal cell wall polysaccharides (Fig. 12). In order to investigate that binding of $(KW)_4$ to the fungal surface occurred via interaction with laminarin or mannan, which are the major components of the fungal cell wall. The MIC concentration of $(KW)_4$ was incubated at different concentrations of polysaccharides and then mixture was tested for anti-candida activity in agar (Fig. 12A) or radial diffusion assay (Fig 12B). As a result, its activity was not inhibited as the amount of polysaccharide increased in the mixture. Agains as with intact $(KW)_4$, CD spectroscopy showed that $(KW)_4$ displayed no major conformational changes associated with polysaccharides laminarin or mannan (Fig. 12C).

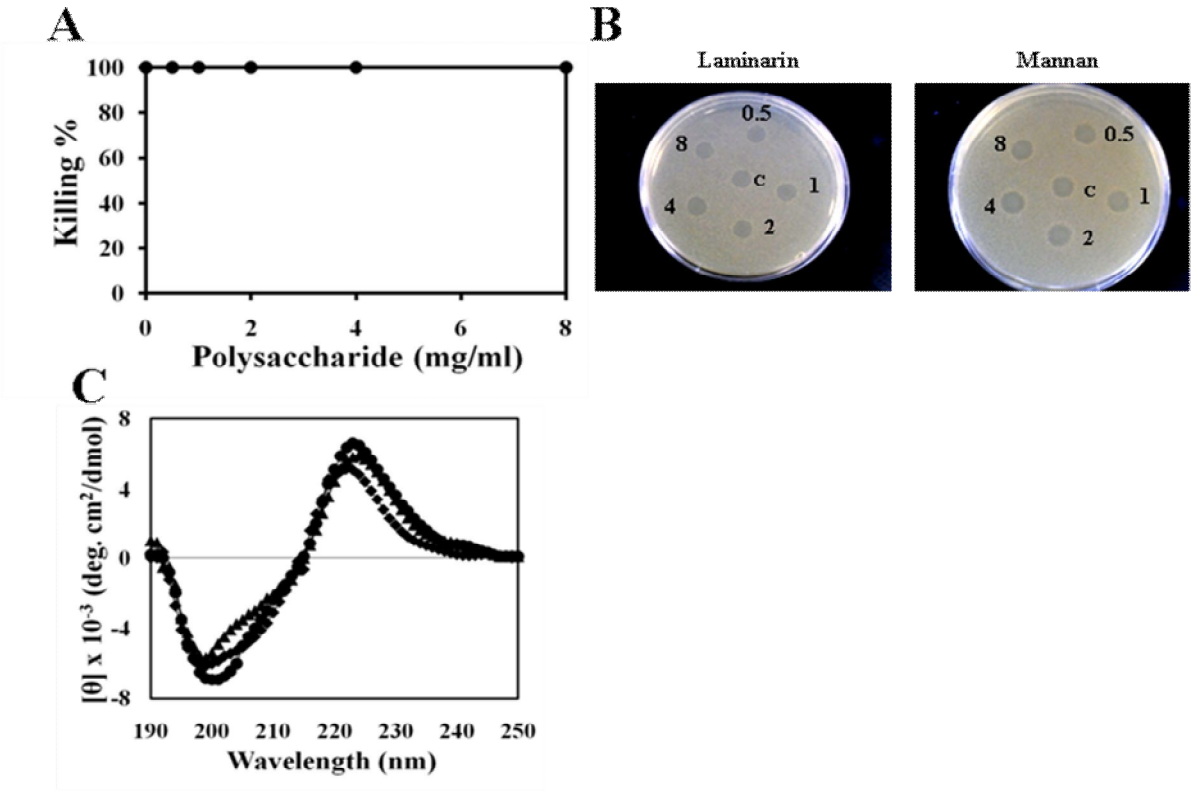

Figure 12. Non-binding of $(KW)_4$ to laminarin or mannan. The anti-candida activities of $(KW)_4$ in the mixture graphed against concentration of polysaccharides (A). Radial diffusion assay was performed by mixing various amounts of laminarin or mannan with 8 μM of $(KW)_4$ in a final volume of 8 μl. The mixture of $(KW)_4$ with laminarin or mannan were introduced into the wells of radial diffusion assay plates seeded with *C. albicans* (B). Numbers represent the polysaccharide concentrations (mg/ml) of the mixture loaded in each well. 8 μl of 8 μM $(KW)_4$ was used for polysaccharides free control (c, control). CD spectroscopy of $(KW)_4$ under different conditions (C). CD spectra for 50 μM of $(KW)_4$ in PBS (■) and in presence of *S. cerevisiae* mannan (●) or laminaria digitata laminarin (▲).

(5) Non-permeabilizing action of peptides in membranes

The dye $DiSC_3$-5 and sytox green were used to demonstrate that AMPs induced cell permeation. Near to sub-MIC or MIC concentration, membrane potential was not observed by these peptides (Fig. 13A). Time course analysis of Sytox-Green uptake was conducted after the addition of peptides to the cells; it also revealed difference between melittin and $(KW)_n$ peptides (Fig. 13B). Melittin had complete memebrane permeabilization within 35 minutes, whereas $(KW)_n$ peptides had no dye infux, suggesting that the diferent mechanism of antifungal activity. The rate of membrane permeabilization was increased with increasing concentration of melittin.

Next, the ability of these peptides was determined to permeabilize the cytoplasmic membrane of *C. albicans* using the fluorescent probes PI. The results of intracellular PI measurements were analysed by fluorescence microscopy and are displayed in figure 13C. They indicate the inability of $(KW)_4$ (8 μM) cause PI permeabilization in *C. albicans* cells after 1 hr incubation. In contrast, cells incubated with the membrane-perturbing antifungal peptide melittin (Fig. 13C3), used as positive control, and showed fluorescence image due to intracellualr PI accumulated indicative of membrane permeabilization.

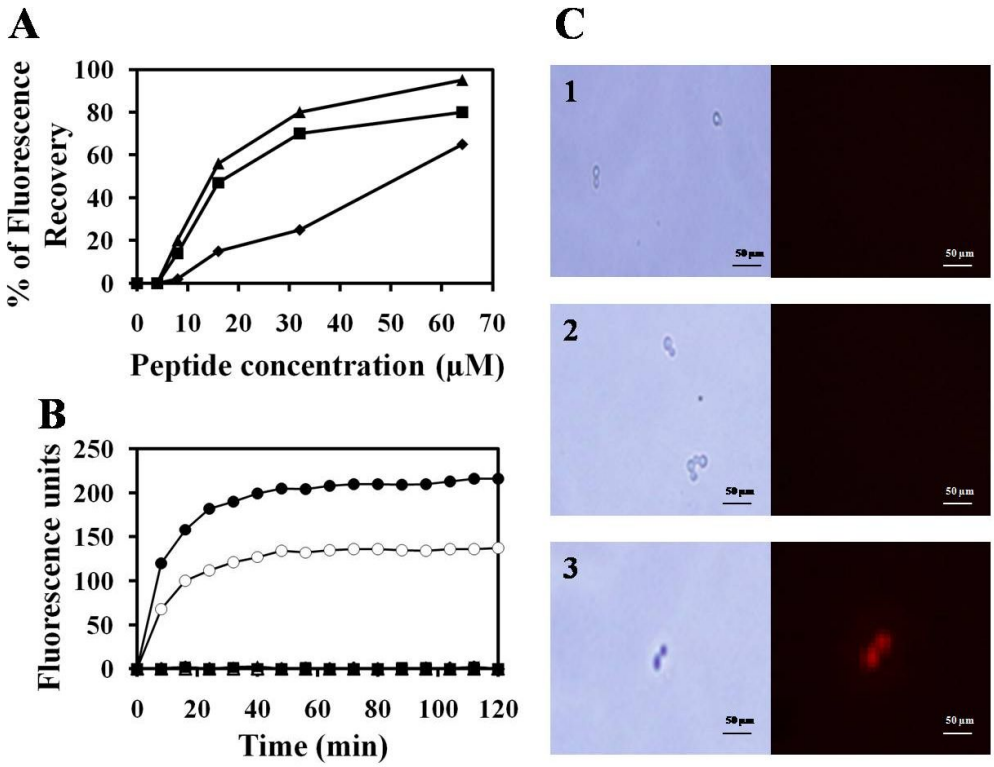

Figure 13. Non-permeabilization of membrane by peptides in cells. The peptides were added to *C. albicans* cells that were pre-equilibrated with the fluorescent dye $DiSC_3$-5 for 60 min. Fluorescense are as follows: $(KW)_3$ (♦), $(KW)_4$ (■) and $(KW)_5$ (▲). The fluorescence increase obtained using 0.1% Triton X-100 was taken as 100% (A). Membrane permeabilization caused by peptides using *C. albicans*. Time course of fluorescence of the SYTOX Green DNA binding dye after uptake of 1 µM SYTOX Green into 2 x 10^7 spore/ml. Peptides ($(KW)_3$ (♦), $(KW)_4$ (■), $(KW)_5$ (▲) and melittin (●)) were added at their sub-MIC (white) or MIC (black) concentrations and the uptake of the dye through the plasma membrane was monitorned by flourescence at an

excitation at 485 nm and emission at 520 nm shows the comparison of SYTOX Green dye leakage in *C. albicans* (B). Fluorescence microscopy of *C. albicans* treated with peptides. *C. albicans* was incubated without peptide or at MIC concentration of peptides (images 1, 2 and 3 represents peptide free control, $(KW)_4$, melittin respectively). After incubation, samples were stained with propidium iodide (PI, 10 μM). Panels represent bright-field images (left) and red flouresence indicative of PI uptake (right) (C).

Cell permeability was monitored by release of the intracellular dye calcein. I determined the ability of these peptides to cause leakage of entrapped calceins from PE:PC:PI:ergosterol at a ratio of 5:4:1:2 (fungal membrane mimetics environments) or PC:CH:SM at a ratio of 1:1:1 (eukaryotic membranes mimetics environments) (Fig. 14). Melittin was most efficient than other peptides, causing 80% and 95% calcein leakage from PE:PC:PI:ergosterol or PC:CH:SM liposomes, respectively, while $(KW)_5$ caused 10% and 60%, respectively**.** $(KW)_3$ and $(KW)_4$ did not caused calcein leakage from any of the liposmes even at 0.1 ratio P/L.

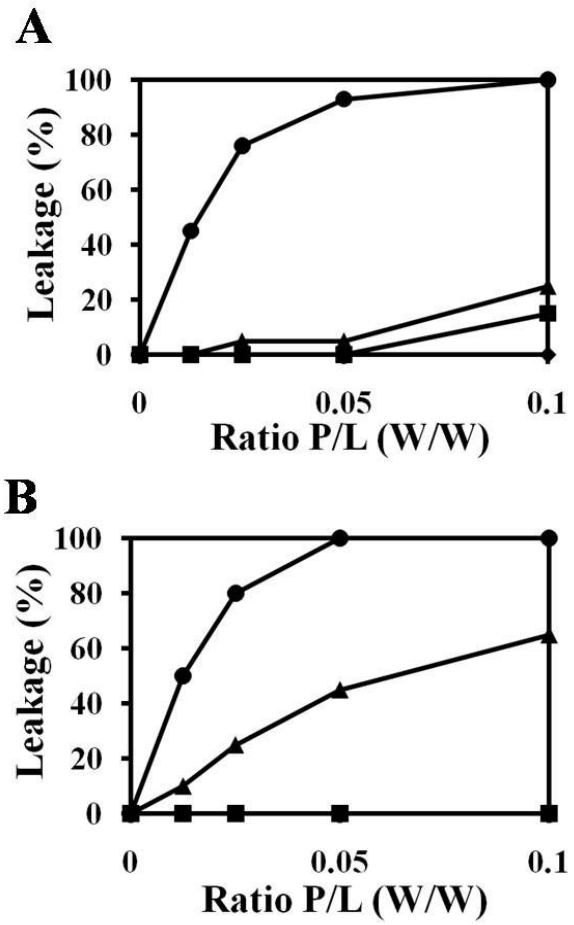

Figure 14. Calcein leakage in PE/PC/PI/ergosterol (A, 5:4:1:2, w/w/w/w) and PC:CH:SM (B, 1:1:1, w/w/w) vesicles. Peptides are designated as follows; $(KW)_3$ (♦), $(KW)_4$ (■), $(KW)_5$ (▲) and melittin (●)

(6) Membrane binding action of peptides with membranes

Peptide binding and partitioning into lipid bilayers was examined by recording the Trp fluorescence emission spectra in the presence of vesicles composed of PE:PC:PI:ergosterol (5:4:1:2, w/w) or PC:CH:SM (1:1:1, w/w). In PE:PC:PI:ergosterol (5:4:1:2, w/w) vesicles, membrane binding ability is increased upon their chain length. In the presence of PC:CH:SM (1:1:1, w/w) vesicles, a blue shift and K_{SV} in the Trp emission of $(KW)_5$ (342 nm and 2.8, respectively) was observed, reflecting their location to more hydrophobic environments [79], which is likely correlates strong effect at inducing calcein leakage from the same synthetic membrane (Fig. 14B). On the other hand, the larger blue shift and smaller K_{SV} value of $(KW)_3$ and $(KW)_4$ were not observed in more hydrophobic environment. Furthermore, larger blue shift and low K_{SV} value of $(KW)_n$ peptide suggested that the Trp side chain partitions preferentially into a more rigid, hydrophobic environment in PE:PC:PI:ergosterol (5:4:1:2, w/w) vesicles than in PC:CH:SM (1:1:1, w/w) vesicles.

The secondary structure of the peptides in aqueous solution and in the presence of lipid membranes were determined (Fig. 15). Random coil spectrum of these peptides in aqueous solution was observed. The $(KW)_3$ peptide did not adopt any secondary structure while longer peptides attained β-sheet conformation in the fungal membrane (Fig. 15A-B). Among them, Only $(KW)_5$ peptide clearly adopted β-sheet conformation in zwitterionic liposomes (Fig. 15C).

All peptides were tested for their vesicle aggregation (fusion) ability using PC:CH:SM (1:1:1) LUVs (Fig. 15D). The $(KW)_3$ and $(KW)_4$ peptides had no significant vesicle aggregation was found in PC:CH:SM (1:1:1) LUVs. Contrast to two

peptides, Only $(KW)_5$ peptide caused a massive increase in the turbidity of the PC:CH:SM LUVs indicating that vesicle aggregation takes place, consistent with its calcein leakage at same ratio (Fig. 14B) and thus cytotoxicity aginst HaCaT cells (Fig. 10A).

Table 4. Tryptophan emission maxima of 2 μM peptides and *K*sv in PBS (pH 7.2) or in the presence of 200 μM PE/PC/PI/ergosterol (5:4:1:2, w/w/w/w) SUVs and 200 μM PC:CH:SM (1:1:1, w/w/w) SUVs

Peptides	λ_{max} buffer (nm)	Blue shift (nm)		*K*sv (M^{-1})[a]		
		PE:PC:PI: ergosterol (5:4:1:2, w/w/w/w)	PC:CH:SM (1:1:1, w/w/w)	Buffer	PE:PC:PI: ergosterol (5:4:1:2, w/w/w/w)	PC:CH:SM (1:1:1, w/w/w)
$(KW)_3$	353	6	1	15	2.8	5.7
$(KW)_4$	353	8	1	14	2.2	5.2
$(KW)_5$	351	10	6	11	2.0	2.7

[a]K_{SV} is the Stern-Volmer constants. K_{SV} (M^{-1}) were determined from the Stern Volmer equation $F_0/F_1 = 1 + K_{SV}$ (Q), where Q is the concentration of quencher (acrylamide). Concentration of the quencher varied from 0.04 to 0.20 M.

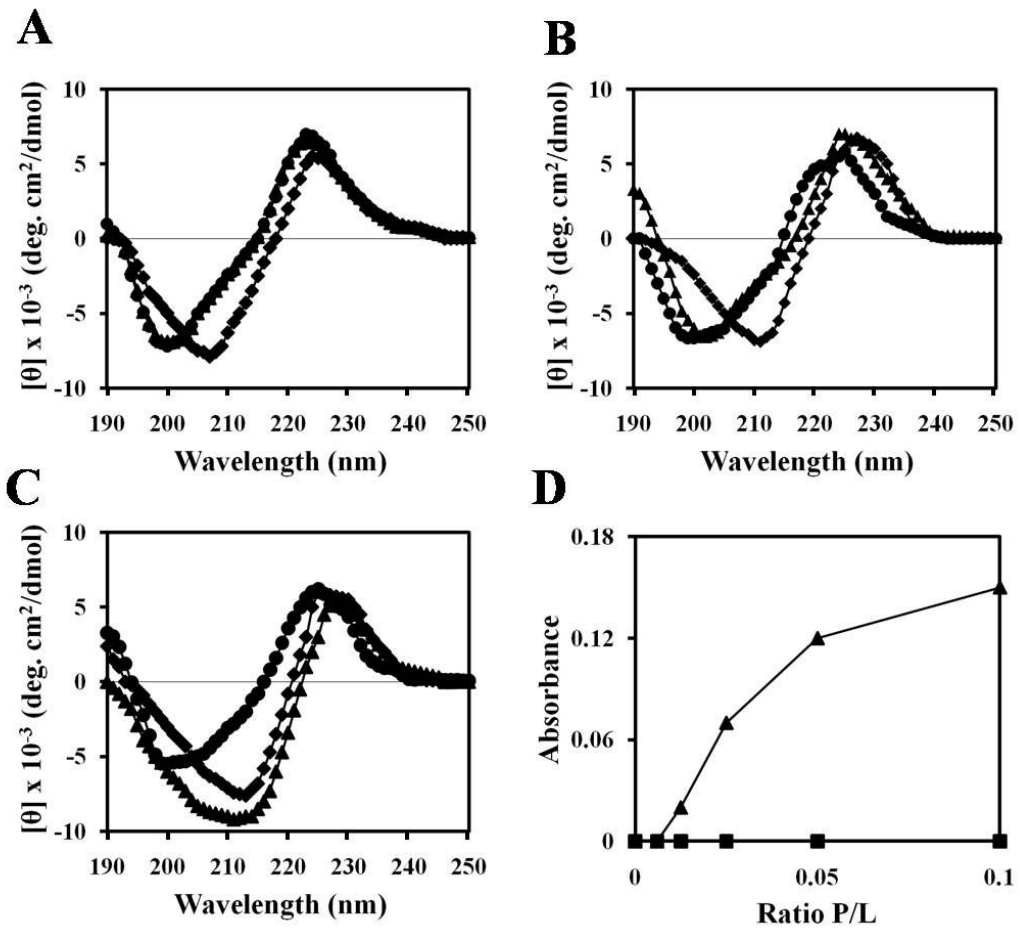

Figure 15. CD spectra of $(KW)_3$ (A), $(KW)_4$ (B) and $(KW)_5$ (C) in the presence of PBS, pH 7.2 (●), PE:PC:PI:ergosterol (5:4:1:2, w/w/w/w) (♦) and PC:CH:SM (1:1:1, w/w/w) (▲) vesicles. LUV aggregation as a function of peptide concentration (D). Peptide solutions were added to a suspension of 400 μM LUVs consisting with PC:CH:SM (1:1:1, w/w/w) vesicles. Aggregation was monitored by absorbance change of LUVs at 405 nm. Peptides are designated as follows; $(KW)_3$ (♦), $(KW)_4$ (■) and $(KW)_5$ (■).

(7) Observation of $(KW)_4$ peptide action in *C. albicans* using Scanning electron microscopy (SEM)

In order to examine the target sites of $(KW)_4$ in *C. albicans*, the cells were treated with $(KW)_4$ of MIC, resulted in no morphological change under SEM (Fig. 16B), which is similar to control cells that displayed a smooth surface (Fig. 16A).

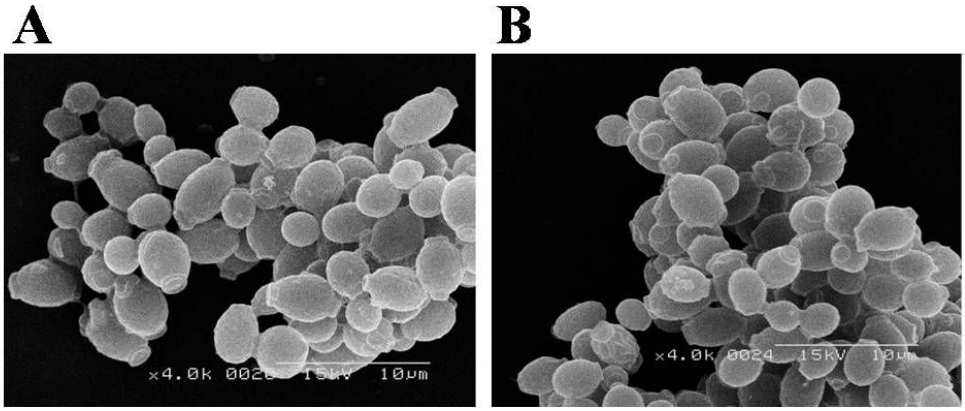

Figure 16. SEM image of *C. albicans* with $(KW)_4$. (A) untreated *C. albicans*, (B) *C. albicans* after treated with $(KW)_4$ of MIC.

(8) Cytoplasmic localization of $(KW)_4$ in *C. albicans*

To determine the target site of $(KW)_4$ prior to intercellualr binding studies, rhodamine labeled-$(KW)_4$ was incubated with *C. albicans* at 1/2X and 1X MIC, after which peptide distribution was visualized by using CLSM (Fig. 17). Rhodamine-$(KW)_4$ peptide penetrated into the cytoplasm of *C. albicans*. Eventhough, rhodamine-$(KW)_4$ at 1/2X the MIC accumualted more on the cytoplasm than plasma membrane. This results indicated that the nucleic acid in the cytoplasm might be the target site for killing action of fungi by $(KW)_n$-series peptides.

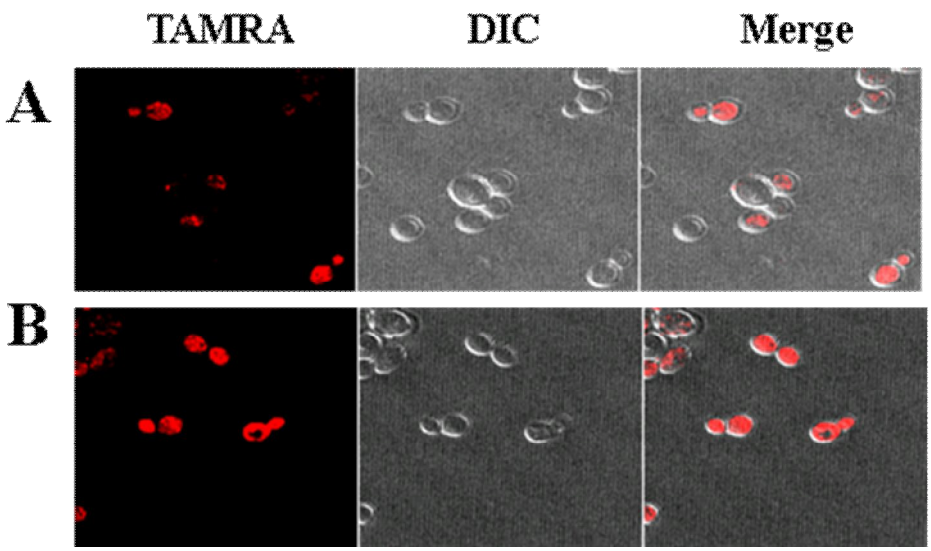

Figure 17. Confocal laser scanning microscopy images of *C. albicans* with rhodamine labeled $(KW)_4$. The cells were reacted with sub MIC (A) or MIC (B) of $(KW)_4$ for 10 minutes in PBS buffer.

(9) Nucleic acid-binding properties of $(KW)_n$ peptides

To estimate RNA-binding ability of these peptides, retardation assay were used (Fig. 18). The $(KW)_5$ with +6 charge showed more affinity for RNA than $(KW)_4$ with +5 charges and $(KW)_3$ with +4 charges. The chain length of the $(KW)_n$ peptides strongly correlates with RNA binding affinity. All peptides binds with RNA at higher weight ratio, binding activity coupled with their chain length. At higher weight ratio, complete retardation of RNA was observed for all peptides. Magainin II, typical membrane active antimicrobial peptides (as a control) at a weight ratio of 1.5 a fraction the RNAs was still able to migrate into the gel, consistent with previous studies [81].

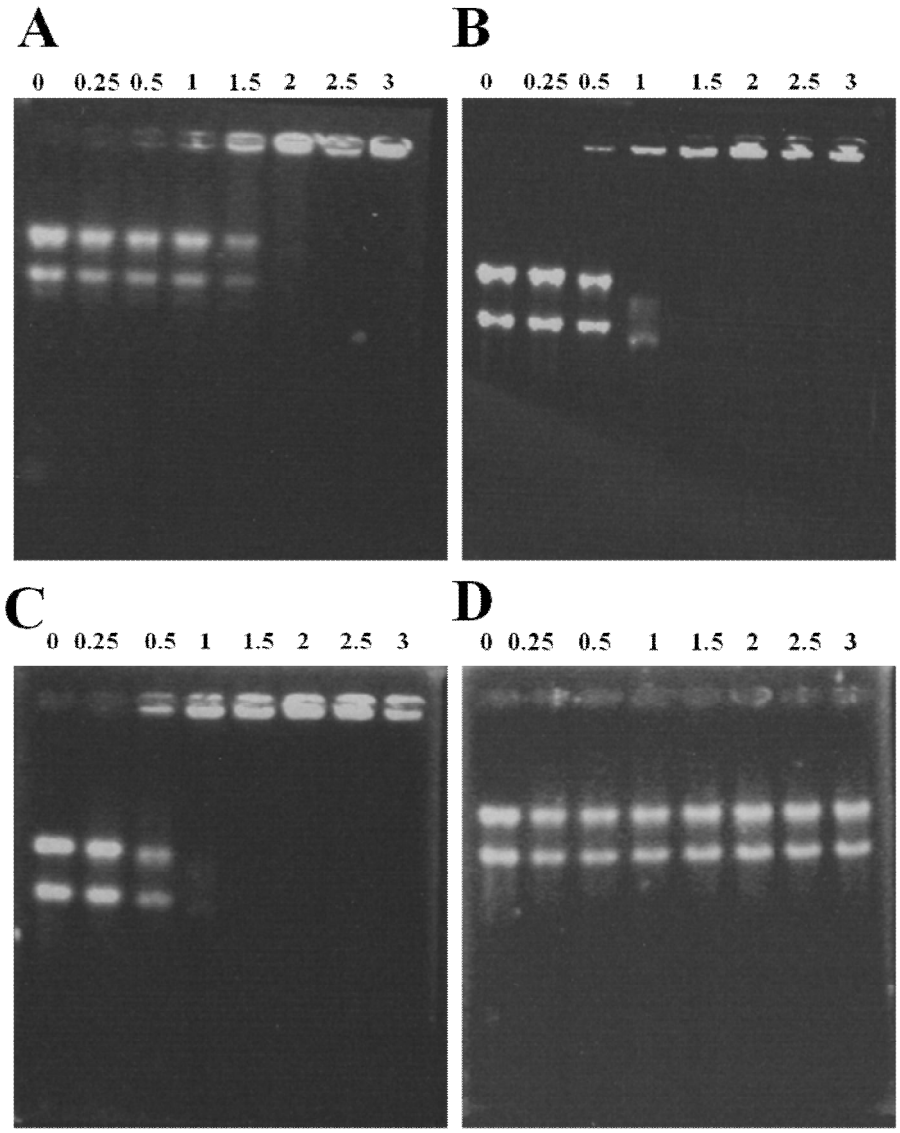

Figure 18. Gel retardation analysis of the binding of peptides to RNA (*C. albicans*). The top panel show different mixtures of peptides (0, 0.5, 1, 2, 3, 4, 5 and 6 µg) and RNA (2 µg). Designations are as follows; $(KW)_3$ (A), $(KW)_4$ (B), $(KW)_5$ (C) and magaini-II (D). Peptide:RNA (weight ratio), magainin-II was used as a negative control.

4. Discussion

The previous study showed that incremental of chain length in the $(RW)_n$ series, enhanced the antibacterial and hemolytic activities [33]. In contrast, other study reported that increasing of chain length in the H-$(LARL)_3$-(LRAL)*n* scrambled peptide was correlated with decreasing antibacterial activity, whereas the reverse situation was found for hemolytic activity [82]. In this study, the improvement of antibacterial activity from peptide $(KW)_2$ to peptide $(KW)_4$ is explained due to the increasing peptide length with an increasing of cationicity and hydrophobicity. In contrast, further increasing cationicity and hydrophobicity, such as in $(KW)_5$ causes the peptide to become weaker than the $(KW)_4$, resulting in a decrease of antibacterial activity as a function of aggregation ability in SP buffer (data not shown). However, in PBS, the $(KW)_5$ and $(KW)_4$ have similar activity against all bacterial strains except *S. typhimurium* and *P. aeruginosa* (Table 1). The overall results suggest that the $(KW)_5$ are soluble, but weakly self-aggregated in PBS solution (Fig. 2). Several studies highlight the hypothesis of self-aggregation state, or increasing hydrophobic interactions of peptides in aqueous solution resulting in a crucial factor for hemolytic activity [83,84]. These hypotheses were consistent with the $(KW)_5$ peptide which shows 71% hemolytic activity at 200 μM (Table 1). Therefore, $(KW)_5$ peptide loses its selective activity for bacterial membrane, but only $(KW)_4$ peptide seems consistent with the balancing of cationicity and hydrophobicity in the AMPs may be the reason to shows broad-spectrum antibacterial activity without hemolytic [85,86].

It has been suggested that this family of scrambled peptide acts by passive engagement with the bacterial surface through KW motifs interactions, as shown by CLSM (Fig. 3). Therefore, I likely assumed that the presence of Lys and Trp residues in

these short peptides may attack bacteria via membrane permeabilization rather than nucleic acid binding mechanism**.** Before studying membrane permeabilization mechanism, their LPS binding property was investigated because AMPs need to traverse the LPS layer of the outer membrane before gaining access to the inner cytoplasmic membrane in Gram-negative bacteria. For some AMPs are largely inactive against Gram-negative pathogen due to the restricted them from LPS physical barrier [87,88], whereas others can overcome this barrier and reaching the inner cytoplasmic membrane [89,90]. From this study indicated that peptides bind to LPS (Fig. 4), thereby suggesting peptide ability to traverse the LPS layer is the main and intial step govering their reaching and premeating the inner membrane, including initiating their antibacterial activity. Next, the bacterial membrane permeation was examined with the help of two methods: (1) monitoring depolarization of membrane potential using $DiSC_3$-5 (2) observing the entry of SYTOX Green dye into cells. The data revealed that the $(KW)_4$ and $(KW)_5$ peptides show similar ability to dissipate the membrane potential of intact *E. coli* and *S. aureus* cells, indicating that the target of the peptides is the cytoplasmic membrane (Fig. 5A-B). Large scale membrane permeability on the *E. coli* and *S. aureus* was observed by the entry of SYTOX Green dye into cells (Fig. 5C-D). These results suggest that the active peptides of $(KW)_4$ and $(KW)_5$ directly effect on the bacterial inner membrane. In addition**,** I know that time scale of $(KW)_4$ and $(KW)_5$ in membrane permeability assay, more consistent with their bactericidal activity that typically takes 35 min (Fig. 5E-F).

Comparisons of the calcein leakage (Fig. 6) and membrane disruption as well as peptide binding activities between $(KW)_2$ and other peptides indicated that the $(KW)_2$ cannot disrupt the bilayers and are not able to cause membrane permeability might be due to their lower length, $(KW)_3$ was moderately active, but $(KW)_4$ and

$(KW)_5$ were efficient. Therefore, longer peptides (n equals 4 or 5) could be access the inner membrane through binding to negatively charged headgroups of bilayer phospholipids that can be driven by electrostatic interactions from Lys or Arg residues [91,92]. The indole rings of Trp in other AMPs [36] have the tendency to partition into the membrane interface of lipid bilayer region flanking the hydrophobic core [93]. Binding and partition into the lipid bilayer are necessary but not sufficient to cause membrane permeability. For example, The $(KW)_2$ peptide showed reasonable blue shift and low K_{SV} value that reflecting its partition into bilayers but did not significantly cause leakage even at very high peptide to lipid ratio concentrations. Therefore, it was believed that membrane permeabilization was specifically increased by longer peptides. Importantly, these results showed that limitation of peptide length required for membrane permeabilization is the disruption of the lipid packing.

The turbidity assay (Fig. 6C) results indicated that peptides mode of action on the negatively charged bacterial membrane via an aggregation like mechanism. The bacterial aggregation effect may be dependent on the number of electrostatic/hydrophobic interactions in these peptides, such as Lys and Trp residues in the sequences. Therefore, peptide with hydrophobic residues may promote both peptide-peptide and also peptide-lipid interactions. However, interaction of peptide with lipids might be mainly stabilized by attraction of opposite charges. These interactions might be initiated to disturb the lipid-water interface of the membrane, and the presences of interactions are thought to favour the fusion or aggregation effect of liposomes. The aggregation of bacterial cells was observed with peptide as well (Fig. 8B). As these bacterial membrane which could not induced spontaneous aggregation from individual bacterial cells [94]. Therefore, bacterial aggregation must be a result of peptide-charge and peptide-lipid interactions. Some AMPs have previously been

demonstrated via an aggregation-dependent mechanism. For example, antibacterial protein, hydramacin-1 from basal metazoan hydra aggregates liposomes or bacteria through electrostatic and hydrophobic interactions. The results also clearly indicated that hydramacin-1 permeabilizes the bacterial membrane; subsequently change their cell morphology [94]. On the other hand, a parotid secretory protein from saliva aggregates bacteria through hydrophobic interactions that is mainly dependent on the number of amine groups in the peptide [95]. Finally, the CD data revealed that the peptides $(KW)_4$ and $(KW)_5$ have structural conformation in the negatively charged lipid membrane. This is consistent with their respective abilities to disrupt lipid bilayers and a promoting aggregation of liposomes. In addition, the CD spectra of an alternating repeat of polar and non-polar residues that could favour β-sheets have been reported [96,97].

In summary, increasing chain length with increasing ratio between hydrophobicity and the net charge, increased both antibacterial and membrane permeability activities, but, $(KW)_5$ peptide could not increased its activity, probably due to its aggregation state. While for hemolysis activity, increasing peptide length with increasing hydrophobicity by its self aggregation resulted in stronger hemolysis in hRBCs. Based on the results obtained, a schematic representation of the mechanism of action of $(KW)_4$ is proposed (Fig. 19). The findings show that the peptide initially bind to LPS of the outer membrane of Gram negative bacteria and formed a β-sheet conformation (Fig. 4B) due to electrostatic forces with its anionic diphosphoryl head groups, then followed by hydrophobic interactions with its fatty acyl chains. Afterwards, peptide inserts into the inner leaflet lipids of LPS and could translocate to the space between the two bacterial membranes. Where peptide is able to induce fusion of two bacterial membrane, rich in PE and PG by both electrostatic/hydrophobic

interaction (e.g., in *E. coli*), which cause leakage of bacterial contents followed by aggregation of liposomes (PE:PG) as well as bacterial cells reported for $(KW)_4$. This membranolytic peptide may work for resistant bacteria which could be promising in the search for a new class of short scrambled antibacterial peptides.

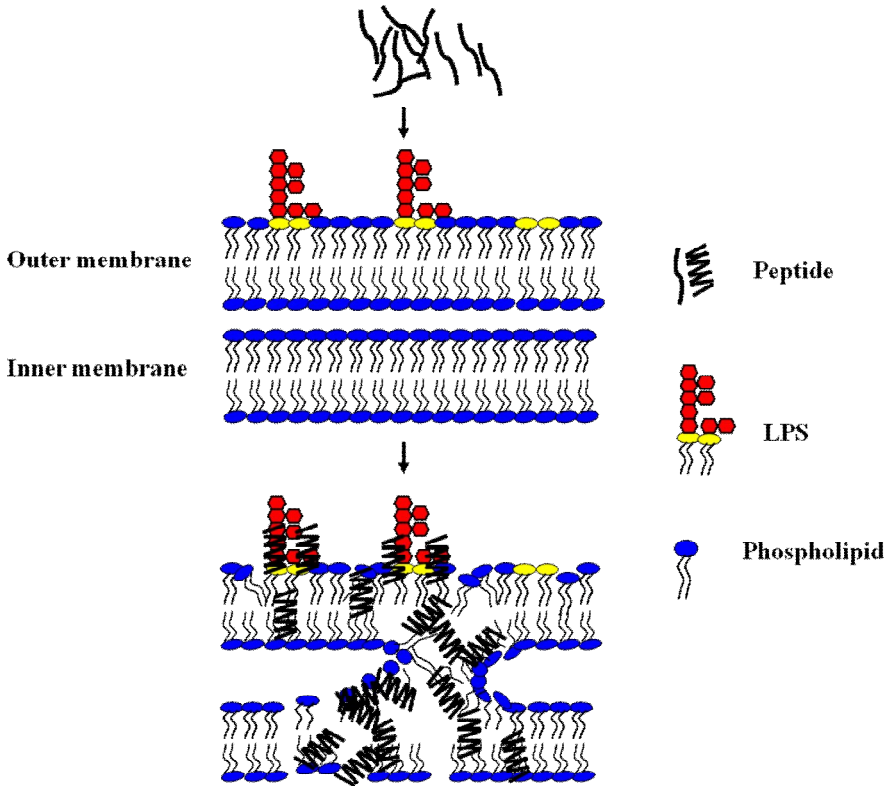

Fig. 19. Schematic representation of the proposed mechanism of action of $(KW)_4$ peptides in bacterial cells. These peptides have electrostatic and hydrophobic interactions with the LPS of the outer leaflet of outer membrane. These interactions allow the peptide insertion and translocation to the inner leaflet lipids of LPS, then binding to the outer leaflets lipids of the inner membrane. At this stage, peptide induces fusion of the inner leaflet of the outer membrane and the inner membrane. These membrane fusion events promote increased membrane permeability with the leakage of the bacterial content, consequently cells were aggregated.

Many of short AMPs are rich in Lys or Arg and Trp with high microbicidal activity (31,33,35,98-100). However, it is not yet clear how these peptides kill fungal cells, but it is widely believed that AMPs kill by disrupting fungal membrane, allowing the leakage of small ions and the larger cytoplasmic components. Therefore, there is a need for clarification of the mechanism of action of these kinds of peptides against *C. albicans* cells. Although, it is thus important to develope optimization of chain length that will be useful for scrambled peptides to favorably interact with fungal membrane and improved their non-toxic to host cells would appear to be most promising candidate for large–scale production.

Here, it was found that antifungal activity of these peptide was generally increased with their chain length, However the shortest chain was relatively inactive, while $(KW)_3$ attained a threshold length in biological response and the two longer chains showed approximate a similar antifungal activity level in PBS. In rich media, $(KW)_3$ had no antifungal activity aginst resistant strains and hyphal condition of *C. albicans*, while longer peptides were capable of exerting its antifungal activity (Table 3). In order to maintain the antifungal activity for these peptides there is a threshold level of cationicity and hydrophobicity. This threshold levels could depend largely on the length of the peptide. Although, the peptide salt insensitivity increased with their chain length. This study confirms that influence length and addition of Trp in a peptide sequence should be preserved for antimicrobial potency in even high salt condition, consistent with previous studies [101].

Anticandida activity of these peptides in low pH (Fig. 9C), suggesting that longer peptides could target *candida* cells in different compartments (e.g., skin and the vagina, cryogenic dental foci, gastric lumen, lung lining fluids in cystic fibrosis and

asthma). It is well known that above orgains of the human body have acidic pH environments [102].

$(KW)_5$ displayed some features that were different from the other peptides, such as the presence of cytotoxicity (Fig. 10A). One possible explanation is that increasing peptide length from $(KW)_4$, self association may cause peptide stacking, creating additional stress on the HaCaT cell membrane and thus inducing cytotoxicity. Studies with $(KW)_5$ showed a correlation between increasing peptide concentration and leads to self association in PBS (Fig. 9D). Therefore, I have identified $(KW)_4$ as a sequence with potential to serve as relatively nontoxic antifungal peptide compared to $(KW)_5$. Also in $(KW)_4$ showed their greater antifungal activity in rich media and salt conditions compared to $(KW)_3$ that can be produced economically on a large scale.

The fungicidal activity of these peptides was confirmed in assays of its killing kinetics with *C. albicans* (Fig. 11). Also, killing activity of these peptides was not depending on active transport mechanism, unlike beta-defension [103]. This data could explain the longer time needed for the peptide to exert its fungicidal activity compared to that of membranolytic peptide that typically takes short minutes to complete the fungicidal activity**,** which suggests that a different effect of these peptides contributes its killing action.

It is well known that compositions of cell wall components are essential for antifungal peptide or protein for its activity against pathogens [63,104,105]. It has been suggested that cell wall components influence internalization and antifungal activity of the Histatin 5 [63]. In case of NAD1, permeabilization of plasma membrane and subsequent entry into target cells is mainly dependent on the cell wall components [105]. Therefore, I likely examined the role of the cell wall polysaccharides in the activity of the peptide. However**,** the presence of $(KW)_4$ with cell wall polysaccharides

could not inhibited its fungicidal activity (Fig. 12A-B). In addition, CD experiment also did not detect any major conformational changes upon interaction with polysaccharides (Fig. 12C). Therefore, it is clearly indicated that cell wall components is not having essential role in fungicidal activity of these peptides. This point is clearly supported that many AMPs killing fungal cells even removal of cell wall components does not inhibited their antifungal activity [105,106]. Apart from cell wall components dependent, killing of fungal cells by antimicrobial peptides has been proposed to occur in two main ways: (i) through disruption of the plasma membrane leading to leakage of cytoplasmic contents or (ii) through interaction with intracellular targets. Therefore, the rate of fungal membranes permeabilization was examined with the help of three methods: 1). Monitoring depolarization of membrane potential using $DiSC_3$-5 2) observing the entry of SYTOX Green or PI dye into cells. However, these peptides showed no significant membrane depolarization at their sub-MIC or MIC concentration (Fig. 13A). This observation is consistent with SYTOX Green uptake assay, indicating non-permeabilization activity towards the fungal membranes by these peptides (Fig. 13B). This conclusion is supported by the comparison with melittin, for which the SG uptake increased with significant permeabilization observed within the first 10 min**.** This supports the hypothesis that this peptides acts by direct interaction with fungal plasma membrane and successively disrupting the membrane to allow the uptake of PI dye that is accumulated within cytoplasmic and can be used as an indicated of plasma membrane permeabilization (Fig. 13C-3). This hypothesis is likely correlated with previous report indicated that exposure of *C. albicans* to melittin causes gross destruction and rupture of plasma membranes [107]. In contrast to melittin, the $(KW)_4$ did not induce the influx of PI into *C. albicans* cells (Fig. 13C-2), indicating non-membrane permeabilizing killing action. This is also supported with other AMPs, at

their minimal fungicidal concentration, there was no indication of peptides killing cell by permeabilizing the fungal membrane [89, 108].

Further support for these peptides modes of action came from calcein leakage studies showed that these peptides did not cause calcein leakage even at very high peptide lipid ratio (Fig. 14). This result is contrast to melittin in this study and other AMPs [109,110] caused calcein leakages from fungal liposomes. Therefore, it seems that these short peptides not only adsorbs on the surface of the vesicles, neutralizing its charge, but also inserts on the membrane, due to hydrophobic interactions. Fluorescent labeling has been used to show internalization of short cationic peptides across model cell membranes [111-114]. However, the peptide/membarne interactions remain important as they can be favourable for peptide translocation across the lipid membrane, even when a peptide is not membrane permeabilizing [115]. This agrees with the proposal that cellular uptake of CPPs is a consequence of its direct translocation through cell membranes, following conformational changes induced by peptide–membrane interactions [116-118]. In this study, the results demonstrated that larger blue shift and smaller K_{SV} value for all three peptides are deeply partition into a more hydrophobic environment in model fungal than zwitetterionic liposomes (Table 4). The high cost of partitioning peptide bonds into the membrane interface is a major driving force for the formation of secondary structure in membrane environments [93, 119,120]. The CD data aslo indicate that all of the three peptides forms β-sheet conformation upon association with the fungal membrane (Fig. 15), and thus also insertion mode befor peptide internalization into cytoplasm. Additionally, these peptides use in this study have weak affinities for membrane containing zwitterinic lipids but only $(KW)_5$ had significant calcein leakage (Fig. 14B), furthermore,

conformation changes (Fig. 15C) and vesicle aggregations (Fig. 15D) induced in the same liposomes.

The data presented here that these peptides had no disruption at both the fungal membrane and artifical similar liposomes (Fig. 13-14); a similar effect was observed with SEM clearly reveals substantial retention of cellular and cytoplasmic integrity of *C. albicans* cells (Fig. 16). This could indicate that peptide action is mainly other targets, possibly intracellular components, such as DNA and RNA, resulting in cell killing. Therefore, the location of fluorescently labeled peptides on live celles was examined by confocal microscopy. This observation showed that peptide internalized into the cytoplasm (Fig. 17), therefore, internalization mechanism of $(KW)_n$ is reasonbly believed that the presence of negatively charged phospholipids containing fungal liposomes enhances the ability of $(KW)_n$ to bind the membrane. In fact, the lysine side chains have possibility to interact with the lipid phosphate groups both electrostatically and by hydrogen bonds. This type of interaction has been localised in the lipid-water interface [91,92]. The Trp residues are also involved in the stabilization of the lipid-peptide complex [36,93]. This stabilization is occurred through van der Waals forces between aromatic residues and hydrophobic lipid chains. Therefore, it is clearly indicated that these peptides interact with and insert into lipid membranes and followed by insertion into the nucleus, and their antifungal potency correlates with the strength of such interactions. Other studies also indicated that membrane interactions are important for the Combi peptides [121,122], confocal microscopy obtained for these peptides show that they can rapidly become localized in the cytoplasm of microbial cells, which suggests that they act on intracellular targets [121,122]. Once peptide inside the nucleus, these peptides then perform other function of affinity to intercellualr targets in the nucleus and these targets that are linked to explain peptide

activity represent a more efficient process of killing cells. Therefore, to test this hypothesis, gel retardation experiment was performed to confirm that a complex was formed when the weight ratio of these peptides to RNAs was 0.3 (Fig. 18). The RNA-binding action of these peptides has been suggets the mechanism of action of these peptides strongly binds to phosphodiester bonds via its positively charged Lys and the Trp should stack between the nucleotide base and ribose in each strand of the RNA duplex. Cationic AMPs with nucleic acid binding properties are known [81,123], as are Trp-rich CAMP such as indolicidin and LfcinB [124,125]. The PAF26 (AC-RKKWFW-NH_2) is one such cell-penetrating peptide and also translocates and accumulate inside fungal cells and binds RNA [126]. This peptide have a remarkable sequence similarity with $(KW)_n$-series peptides, therefore it can be reasonably accepted that $(KW)_n$-series kill the fungai by targeting intracellular component such as RNA, which would be expected to inhibit the intracellular synthesis of nucleic acid and protein.

In conclusion, longer peptides are more effective in killing *C. albicans*, although in the presence of variable salts and pHs did not reduced longer peptide activity. However, increasing peptide length with increasing ratio between hydrophobicity and the net charge resulted in increased cytotoxicity against HaCaT cells. The combined results of whole data allowed us to decipher the mode of action of longer peptides on fungal membrane (Fig. 20). Changes in secondary structure and peptide–membrane interactions are easily followed in a non-membranolytic manner. Peptide-lipid matrix interaction to adopt a beta sheet conformation, this tendency help peptide allow to cytoplasm without cell wall components binding and endocytosis process. The correlation of non-membrane permeabilization kinetics with the location of peptides in the cytosol of *C. albicans* concludes that these peptides appear to

enhance cell killing by interacting with intracellular targets such as RNAs. Such peptides would have increased potency against target fungi, thereby reducing dosage and cost, and rendering them attractive for clinical use.

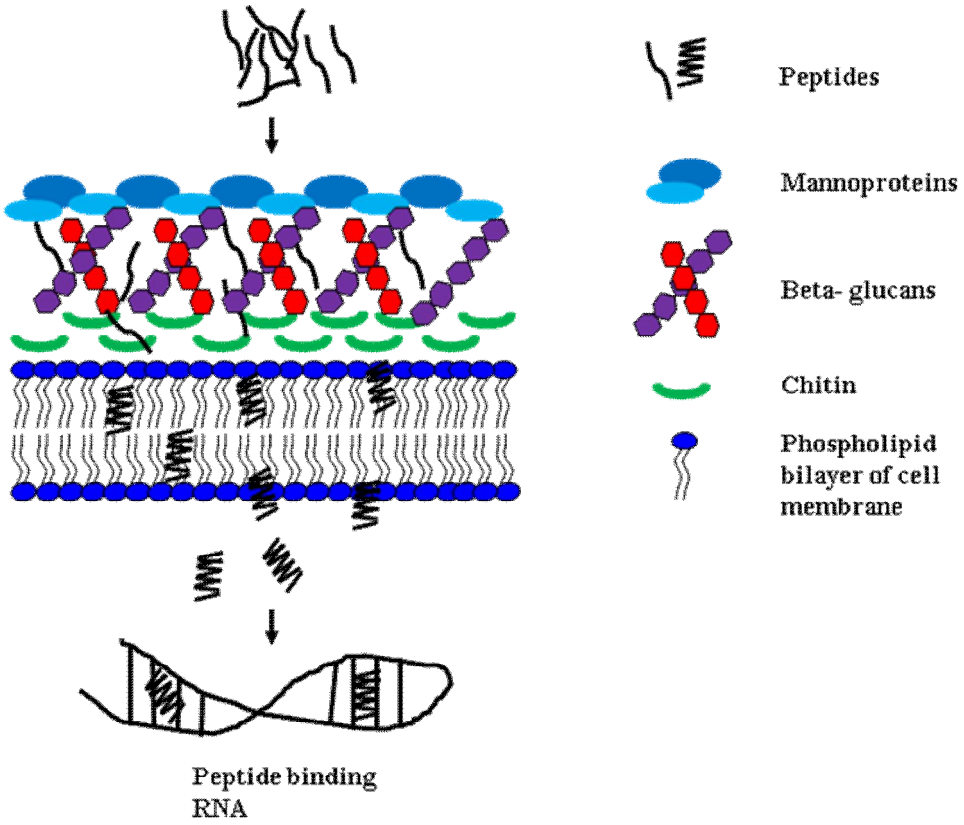

Fig. 20. Schematic representation of the proposed mechanism of action of $(KW)_n$ peptides in fungal cells. The peptide did not interact with cell wall components. In this model peptides bind to a phospholipid membrane, driven by a combination of electrostaic (Lys) and hydrophobic (Trp) interactions. The peptide-membrane interaction to promote peptide assembe into beta sheets in the lipid matrix. In the post-membrane interaction, the peptide is simply diffused towards cytoplasmic targets (nucleic acid target) therefore there is no membrane destabilization and these bilayers do not release their contents.

5. References

[1] R.E. Hancock, The end of an era? Nat. Rev. Drug Discovery 6 (2007) 28.

[2] U. Theuretzbacher, J.H. Toney, Nature's clarion call of antibacterial resistance: are we listening? Curr. Opin. Invest. Drugs 7 (2006) 158-166.

[3] C.V. Paya, Fungal infections in solid-organ transplantation, Clin. Infect. Dis. 16 (1993) 677-688.

[4] A.E. Brown, Overview of fungal infections in cancer patients, Semin. Oncol. 17 (1990) 2-5.

[5] F.M. Durden, B. Elewski, Fungal infections in HIV-infected patients, Semin. Cutan. Med. Surg. 16 (1997) 200-212.

[6] H. Vanden Bossche, D.W. Warnock, B. Dupont, D. Kerridge, S. Sen Gupta, L. Improvisi, P. Marichal, F.C. Odds, F. Provost, O. Ronin, Mechanisms and clinical impact of antifungal drug resistance, J. Med. Vet. Mycol. 32 (1994) 189-202.

[7] H. Tsai, L.A. Bobek, Human salivary histatins: promising antifungal therapeutic agents, Crit. Rev. Oral Biol. Med. 9 (1998) 480-497.

[8] T. Ganz, R.I. Lehrer, Antibiotic peptides from higher eukaryotes: biology and applications, Mol. Med. Today 5 (1999) 292-297.

[9] H. Jenssen, O. Hamill, R.E. Hancock, Peptide antimicrobial agents, Clin. Microbiol. Rev. 19 (2006) 491-511.

[10] J.H. Wong, L. Xia, T.B. Ng, A review of defensions of diverse origins, Curr. Protein Pept. Sci. 8 (2007) 446-459.

[11] G. Bergsson, B. Agerberth, H. Jornvall, G.H. Gudmundsson, Isolation and identification of antimicrobial components from the epidermal mucus of Atlantic cod (*Gadus morhua*), FEBS J. 272 (2005) 4960-4969.

[12] S.-C. Park, M.H. Kim, M.A. Hossain, S.Y. Shin, Y. Kim, L. Stella, J.D. Wade, Y. Park, K.-S. Hahm, Amphipathic α-helical peptide, HP (2-20), and its analogues derived from *Helicobacter pylori*: Pore formation mechanism in various lipid composition, Biochim. Biophys. Acta 1778 (2008) 229-241.

[13] M.R. Yeaman, N.Y. Yount, Mechanism of antimicrobial peptide action and resistance, Pharmacol. Rev. 55 (2003) 27–55.

[14] R.E. Hancock, D.S. Chapple, Peptide antibiotics, Antimicrob. Agents Chemother. 43 (1999) 1317–1323.

[15] J.P. Powers, R.E. Hancock, The relationship between peptide structure and antibacterial activity, Peptides 24 (2003) 1681-1691.

[16] M. Zasloff, Antimicrobial peptides of multicellular organisms, Nature 415 (2002) 389-395.

[17] H.G. Boman, Antibacterial peptides:basic facts and emerging concepts, J. Intern. Med. 254 (2003) 197-215.

[18] R.M. Epand, H.J. Vogel, Diversity of antimicrobial peptides and their mechanisms of action, Biochem. Biophys. Acta 1462 (1999) 11-28.

[19] K. Matsuzaki, Magainins as paradigm for the mode of action of pore forming polypeptides. Biochim. Biophys. Acta, 1376 (1998) 391-400.

[20] E.F. Haney, H.N. Hunter, K. Matsuzaki, H.J. Vogel, Solution NMR studies of amphibian antimicrobial peptides: linking structure to function? Biochim. Biophys. Acta 1788 (2009) 1639-1655.

[21] Shai Y. Mechanism of the binding, insertion and destabilization of phospholipid bilayer membranes by α-helical antimicrobial and cell-selective membrane-lytic peptides, Biochim. Biophys. Acta 1462 (1999) 55-70.

[22] G. Ehrenstein, H. Lecar, Electrically gated ionic channels in lipid bilayers, Q. Rev.

Biophys. 10 (1977) 1-34.

[23] Y. pouny, D. Rapaport, A. Mor, P. Nicolas, Y. Shai, Interaction of antimicrobial dermaseptin and its fluorescently labeled analogues with phospholipid membranes, Biochemistry 31 (1992) 12416-12423.

[24] M.A. Baker, W.L. Maloy, M. Zasloff, L.S. Jacob, Anticancer efficacy of magainin 2 and analogue peptides, Cancer Res. 53 (1993) 3052-3057.

[25] S.A. Johnstones, K. Gelmon, L.D. Mayer, R.E.W. Hancock, M.B. Bally, In vitro characterization of the anticancer activity of membrane active cationic peptides. I. peptide-mediated cytotoxicity and peptide-enhanced cytotoxic activity of doxorubicin against wild-type and *p*-glycoprotein over-expressing tumor cell lines, Anticancer Drug Des. 15 (2000) 151-160.

[26] R.L. Gallo, M. One, T. Povsic, C. Page, E. Eriksson, M. Klagsbrun, M. Bernfield, Syndecans, cell surface heparin sulfate proteoglycans, are induced by a proline-rich from antimicrobial peptide from wounds, Proc. Natl. Acad. Sci. USA 91 (1994) 11035-11039.

[27] R.E. Hancock, H.G. Sahl, Antimicrobial and host-defense peptides as new anti-infective therapeutic strategies, Nat. Biotechnol. 24 (2006) 1551-1557.

[28] Y. Shai, J. Fox, C. Caratsch, Y.L. Shih, C. Edwards, P. Lazarovici, Sequencing and synthesis of pardaxin, a polypeptide from the Red Sea Moses sole with ionophore activity, FEBS Lett. 242 (1988) 161-166.

[29] Z. Oren, Y. Shai, Selective lysis of bacteria but not mammalian cells by diastereomers of melittin: structure-function study, Biochemistry 36 (1997) 1826-1835.

[30] J. Johansson, G.H. Gudmundsson, M.E. Rottenberg, K.D. Berndt, B. Agerberth, Conformation dependent antibacterial activity of the naturally occurring human peptide LL-37, J. Biol. Chem. 273 (1998) 3718-3724.

[31] M.B. Strom, O. Rekdal, J.S. Svendsen, Antimicrobial activity of short arginine- and tryptophan-rich peptides, J. Pept. Sci. 8 (2002) 431-437.

[32] M.B. Storm, B.E. Haug, M.L. Skar, W. Stensen, T. Stiberg, J.S. Svendsen, The pharmacophore of short cationic antibacterial peptides, J. Med. Chem. 46 (2003) 1567-1570.

[33] Z. Liu, A. Brady, A. Young, B. Rasimick, K. Chen, C. Zhou, N.R. Kallenbach, Length effects in antimicrobial peptides of the $(RW)_n$ series, Antimicrob. Agents Chemother. 51 (2007) 597-603.

[34] W. Jing, H.N. Hunter, J. Hagel, H.J. Vogel, The structure of the antimicrobial peptide Ac-RRWWRF-NH_2 bound to micelles and its interactions with phospholipids bilayers, J. Pept. Res. 61(2003) 219-229.

[35] M. Dathe, H. Nikolenko, J. Klose, M. Bienert, Cyclization increases the antimicrobial activity and selectivity of arginine- and tryptophan- containing hexapeptides, Biochemistry 43 (2004) 9140-9150.

[36] D.J. Schibli, R.F. Epand, H.J. Vogel, R.M. Epand, Tryptophan-rich antimicrobial peptides: comparative properties and membrane interactions, Biochem. Cell Biol. 80 (2002) 667-677.

[37] W. Bellamy, M. Takase, H. Wakabayashi, K. Kawase, M. Tomita, Antibacterial spectrum of lactoferricin-B, a potent bactericidal peptide derived from the N-terminal region of bovine lactoferrin, J. Appl. Bacteriol. 73 (1992) 472-479.

[38] D.J. Schibli, P.M. Hwang, H.J. Vogel, Structure of the antimicrobial peptide tritrpticin bound to micelles: a distinct membrane bound peptide fold,

Biochemistry 38 (1999) 16749-16755.

[39] M.E. Selsted, M.J. Novotny, W.L. Morris, Y.Q. Tang, W. Smith, J.S. Cullor, Indolicidin, a novel bactericidal tridecapeptide amide from neutrophils, J. Biol. Chem. 267 (1992) 4292-4295.

[40] P. Staubitz, A. Peschel, W. F. Nieuwenhuizen, M. Otto, F. Gotz, G. Jung, R. W. Jack, Structure-function relationships in the tryptophan-rich, antimicrobial peptide Indolicidin, J. Pept. Sci. 7 (2001) 552-564.

[41] M.B. Strom, B.E. Haug, O. Rekdal, M.L. Skar, W. Stensen, J.S. Svendsen, Important structural features of 15-residue lactoferricin derivatives and methods for improvement of antimicrobial activity, Biochem. Cell Biol. 80 (2002) 65-74.

[42] H.J. Vogel, D.J. Schibli, W.G. Jing, E.M. Lohmeier-Vogel, R.F. Epand, R.M. Epand, Towards a structure-function analysis of bovine lactoferricin and related tryptophan- and arginine-containing peptides, Biochem. Cell Biol. 80 (2002) 49-63.

[43] S.T Yang, S.Y. Shin, Y.C. Kim, Y. Kim, K.S. Hahm, J.I. Kim, Conformation-dependent antibiotic activity of tritrpticin, a cathelicidin-derived antimicrobial peptide, Biochem. Biophys. Res. Commun. 296 (2002) 1044–1050.

[44] V.V. Andrushchenko, H.J. Vogel, E.J. Prenner, Interaction of tryptophan-rich cathelicidin antimicrobial peptides with model membranes studied by differential scanning calorimetry, Biochem. Biophys. Acta 1768 (2007) 2447-2458.

[45] C. Subbalakshmi, E. Bikshapathy, N. Sitaram, R. Nagaraj, Antibacterial and hemolytic activities of single tryptophan analogs of indolicidin, Biochem. Biophys. Res. Commun. 274 (2000) 714-716.

[46] S.T. Yang, S.Y. Shin, C.W. Lee, Y.C. Kim, K.S Hahm, J.I. Kim, Selective cytotoxicity following Arg-to-Lys substitution in tritrpticin adopting a unique amphipathic turn structure, FEBS Lett. 540 (2003) 229-233.

[47] J. Andra, D. Monreal, G. Martinez de Tejada, C. Olak, G. Brezesinski, S.S Gomez, T. Goldmann, R. Bartels, K. Brandenburg, I. Moriyon, Rationale for the design of shortened derivatives of the NK-lysine derived antimicrobial peptide NK-2 with improved activity against Gram-negative pathogens, J. Biol. Chem. 282 (2007) 14719-14728.

[48] M. Dathe, M. Schumann, T. Wieprecht, A. Winkler, M. Beyermann, E. Krause, K. Matsuzaki, O. Murase, M. Bienert, Peptide helicity and membrane surface charge modulate the balance of electrostatic and hydrophobic interactions with lipid bilayers and biological membranes, Biochemistry 35 (1996) 12612-12622.

[49] Y.M. Song, Y. Park, S.S. Lim, S.T. Yang, E.R. Woo, I.S. Park, J.S. Lee, J.I. Kim, K.S. Hahm, Y. Kim, S.Y. Shin, Cell selectivity and mechanism of action of antimicrobial model peptides containing peptoid residues, Biochemistry 44 (2005) 12094-12106.

[50] R. Gopal, S.C. Park, K.J. Ha, S.J. Cho, S.W. Kim, P.I. Song, J.W. Nah, Y. Park, K.S. Hahm, Effect of leucine and lysine substitution on the antimicrobial activity and evaluation of the mechanism of the HPA3NT3 analog peptide, J. Pept. Sci. 15 (2009) 589-594.

[51] M.F. Ali, A. Soto, F.C. Knoop, J.M, Conlon, Antimicrobial peptides isolated from skin secretions of the diploid frog, Xenopus tropicalis (Pipidae), Biochem. Biophys. Acta 1550 (2001) 81-89.

[52] D.M. Rothstein, P. Spacciapoli, L.T. Tran, T. Xu, F.D. Roberts, M. Dalla Serra, D.K. Buxton, F.G. Oppenheim, P. Friden, Anticandida activity is retained in p-113,

a 12-amino-acid fragment of histatin 5, Antimicrob. Agents Chemother. 45 (2001) 1367-1373.

[53] Y.S. Koo, J.M. Kim, I.Y. Park, B.J. Yu, S.A. Jang, K.S. Kim, C.B. Park, J.H. Cho, S.C. Kim, Structure-activity relations of parasin I, a histone H2A-derived antimicrobial peptide, peptides 29 (2008) 1102-1108.

[54] W.C. Shen, H.J. Ryser, Conjugation of polyl-lysien to albumin and horseradish peroxidase: a novel method of enhancing the cellular uptake of protrins, Proc Natl. Acad Sci USA, 75 (1978) 1872-1876.

[55] S. Hyun, H.J. Kim, N.J. Lee, K.H. Lee, Y. Lee, D.R. Ahn, K. Kim, S. Jeong, J. Yu, Alpha-helical peptide containing N,N-dimethyl lysine residues displays low-nanomolar and highly specific binding to RRE RNA, J. Am. Chem. Soc. 129 (2007) 4514-4515.

[56] E. Atherton, R.C. Sheppard, Solid Phase Peptide Synthesis, A Practical Approach. IRL: Oxford, 1989.

[57] Y. Pouny, Y. Shai, Interaction of D-amino acid incorporated analogues of pardaxin with membranes, Biochemistry 31 (1992) 9482-9490

[58] Y. Park, D.G. Lee, S.H Jang, E.R. Woo, H.G. Jeong, C.H. Choi, K.S Hahm, A Leu-Lys-rich antimicrobial peptide: activity and mechanism, Biochim. Biophys. Acta, 1645 (2003) 172-182.

[59] S.C. Park, J.R. Lee, S.O. Shin, Y. Park, S.Y. Lee, K.S. Hahm, Characterization of heat-stable protein with antimicrobial activity from *Arabidopsis thaliana*, Biochem. Biophys. Res. Commun. 362 (2007) 562-567.

[60] W.S. Jang, X.S. Li, J.N. Sun, M. Edgerton, The P-113 fragment of histatin 5 requires a specific peptide sequence for intracellular translocation in C*andida albicans*, which is independent of cell wall binding, Antimicrob. Agents

Chemother, 52 (2008) 497-504.

[61] A. Lupetti, A. Paulusma-Annema, M.M. Welling, S. Senesi, J.T. van Dissel, P.H. Nibbering, Candidacidal activities of human lactoferrin peptides derived from the N terminus, Antimicrob. Agents Chemother, 44 (2000) 3257–3263.

[62] R.A. Moore, N.C. Bates, R.E.W. Hancock, Interaction of polycationic antibiotics with *Pseudomonas aeruginosa* lipopolysaccharide and lipid A studied by using dansyl-polymyxin, Antimicrob. Agents Chemother, 29 (1986) 496-500.

[63] W.S. Jang, J.S. Bajwa, J.N. Sun, M. Edgerton. Salivary histatin 5 internalization by translocation, but not endocytosis, is required for fungicidal activity in *Candida albicans*, Mol. Microbiol. 77 (2010) 354-370.

[64] W.S. Jang, H.K. Kim, K.Y. Lee, S.A. Kim, Y.S. Han, I.H. Lee, Antifungal activity of synthetic peptide derived from halocidin, antimicrobial peptide from the tunicate, Halocynthia aurantium, FEBS Lett. 580 (2006) 1490-1496.

[65] N. Papo, Z. Oren, U. Pag, H.G. Sahl, Y. Shai, The consequence of sequence alternation of an amphipathic α-helical antimicrobial peptide and its diastereomers, J. Biol. Chem. 277 (2002) 33913-33921.

[66] N. Sal-Man, Z. Oren, Y. Shai, Preassembly of membrane-active peptides is an important factor in their selectivity toward target cells, Biochemistry 41 (2002) 11921-11930.

[67] M.L. Mangoni, N. Papo, D. Barra, M. Simmaco, A. Bozzi, A. Di Giulio, A.C. Rinaldi, Effects of the antimicrobial peptide temporin L on cell morphology, membrane permeability and viability of *Escherichia coli*, Biochem. J. 380 (2004) 859-865.

[68] P.C. Dewan, A. Anantharaman, V.S. Chauhan, D. Sahal, Antimicrobial action of prototypic amphipathic cationic decapeptides and their branched dimers, Biochemistry 48 (2009) 5642-5657.

[69] D.G. Lee, H.N. Kim, Y. Park, H.K. Kim, B.H. Choi, C.H. Choi, K.S. Hahm, Design of novel analogue peptides with potent antibiotic activity based on the antimicrobial peptide, HP (2-20), derived from N-terminus of *Helicobacter pylori* ribosomal protein L1, Biochem, Biophys. Acta 1598 (2002) 185-194.

[70] L.D. Mayer, M.J. Hope, P.R. Cullis, Vesicles of variable sizes produced by a rapid extrusion procedure, Biochem. Biophys. Acta 858 (1986) 161-168.

[71] J.C.M. Stewart, Colorimetric determination of phospholipids with ammonium ferrothiocyanate, Anal. Biochem. 104 (1980) 10-14.

[72] K. Matsuzaki, K. Sugishita, K. Miyajima, Interactions of an antimicrobial peptide, magainin 2, with lipopolysaccharide-containing liposomes as a model for outer membranes of Gram-negative bacteria, FEBS Lett. 449 (1999) 221-224.

[73] Z. Oren, J.C. Lerman, G.H. Gudmundsson, B. Agerberth, Y. Shai, Structure and organization of the human antimicrobial peptide LL-37 in phospholipid membranes: relevance to the molecular basis for its non-cell-selective activity, Biochem. J. 341 (1999) 501-513.

[74] S.C. Park, J.Y. Kim, S.O. Shin, C.Y. Jeong, M.H. Kim, S.Y. Shin, G.W. Cheong, Y. Park, K.S. Hahm, Investigation of toroidal pore and oligomerization by melittin using transmission electron microscopy, Biochem. Biophys. Res. Commun. 343 (2006) 222-228.

[75] D. Mao, B.A. Wallace, Differential light scattering and adsorption flattening optical effects are minimal in the circular dichroism spectra of small unilamellar vesicles, Biochemistry 23 (1984) 2667-2673.

[76] Y. Rosenfeld, N. Lev, Y. Shai, Effect of the hydrophobicity to net positive charge ratio on antibacterial and anti-endotoxin activities of structurally similar antimicrobial peptides, Biochemistry 49 (2010) 853-861.

[77] R.W. Woody, Contributions of tryptophan side chains to the far-ultraviolet circular dichroism of proteins, Eur. Biophys. J. 23 (1994) 253-262.

[78] A.S. Ladokhin, M.E. Selsted, S.H. White, Bilayer interactions of indolicidin, a small antimicrobial peptide rich in tryptophan, proline, and basic amino acids, Biophys. J. 72 (1997) 794-805.

[79] E.A. Burstein, N.S. Vendenkina, M.N. Ivkova, Fluorescence and the location of tryptophan reisdue in protein molecules, Photochem. photobiol. 18 (1973) 263-279.

[80] W.C. Wimley, T.P. Creamer, S.H. White, Solvation energies of amino acid side chains and backbone in a family of host guest pentapeptides, Biochemistry 35 (1996) 5109-5124.

[81] C.B. Park, H.S. Kim, S.C. Kim, Mechanism of action of the antimicrobial peptide buforin II: buforin II kills microorganisms by penetrating the cell membrane and inhibiting cellular functions, Biochem. Biophys. Res. Commun 244 (1998) 253-257.

[82] T. Niidome, N. Matsuyama, M. Kunihara, T. Hatakeyama, H. Aoyagi, Effect of chain length of cationic model peptides on antibacterial activity, Bull. Chem. Soc. Jpn. 78 (2005) 473-476.

[83] R. Feder, A. Dagan, A. Mor, Structure-activity relationship study of antimicrobial dermaseptin S4 showing the consequences of peptide oligomerization on selective cytotoxicity, J. Biol. Chem. 275 (2000) 4230-4238.

[84] M.M. Javadpour, M.D. Barkley, Self-assembly of designed antimicrobial peptides in solution and micelles, Biochemistry 36 (1997) 9540-9549.

[85] M.M. Javadpour, M.M. Juban, W.C. Lo, S.M. Bishop, J.B. Alberty, S.M. Cowell, C.L. Becker, M.L. McLaughlin, De novo antimicrobial peptides with low mammalian cell toxicity, J. Med. Chem. 39 (1996) 3107-3113.

[86] S. Fernandez-Lopez, H.S. Kim, E.C. Choi, M. Delgado, J.R. Granja, A. Khasanov, K. Kraehenbuehl, G. Long, D.A.Weinberger, K.M. Wilcoxen, M.R. Ghadiri, Antibacterial agents based on the cyclic D,L-α-peptide architecture, Nature 412 (2001) 452-455.

[87] N. Papo, Shai Y, A molecular mechanism for lipopolysaccharide protection of Gram-negative bacteria from antimicrobial peptides, J. Biol. Chem. 280 (2005) 10378-10387.

[88] S.A. Loutet, R.S. Flannagan, Kooi C, P.A. Sokol, M.A. Valvano, A complete lipopolysaccharide inner core oligosaccharide is required for resistance of Burkholderia cenocepacia to antimicrobial peptides and bacterial survival in vivo, J. Bacteriol. 188 (2006) 2073-2080.

[89] S. Farnaud, C. Spiller, L.C. Moriarty, A. Patel, V. Gant , E.W. Odell, R.W. Evans, Interaction of lactoferricin-derived peptides with LPS and antimicrobial activity, FEMS Microbiol. Lett. 233 (2004) 193-199.

[90] S. Bhattachariya, A. Ramamoorthy, Multifunctional host defense peptides: functional and mechanistic insights from NMR structures of potent antimicrobial peptides, FEBS J, 276 (2009) 6465-6473.

[91] A.H. Juffer, C.M. Shepherd, H.J. Vogel, Protein-membrane electrostatic interactions: applications of the lekner summation technique, J. Chem. Phy. 114 (2001) 1892-1905.

[92] C.M. Shepherd, K.A. Schaus, H.J. Vogel, A.H. Juffer, Molecular dynamics study of peptide-bilayer adsorption, Biophys. J. 80 (2001) 579-596.

[93] W.C. Wimley, S.H. White, Experimentally determined hydrophobicity scale for proteins at membrane interfaces, Nat. Struct. Biol. 3 (1996) 842-848.

[94] S. Jung, A.J. Dingley, R. Augustin, F.A. Erxleben, M. Stanisak, C. Gelhaus, T. Gutsmann, M.U. Hammer, R. Podschun, A.M. Bonvin, M. Leippe, T.C. Bosch, J. Grotzinger, Hydramacin-1, structure and antibacterial activity of a protein from the basal metazoan hydra, J. Biol. Chem. 284 (2009) 1896-1905.

[95] S.U. Gorr, J.B. Sotsky, A.P. Shelar, D.R. Demuth, Design of bacteria-agglutinating peptides derived from parotid secretory protein, a number of the bactericidal/permeability increasing-like protein family, Peptides 29 (2008) 2118-2127.

[96] R. Rathinakumar, W.C. Wimley, Biomolecular engineering by combinatorial design and high-throughput screening: small, soluble peptides that permeabilize membranes, J. Am. Chem. Soc. 130 (2008) 9849-9858.

[97] R. Rathinakumar, W.F. Walkenhorst, W.C. Wimley, Broad-spectrum antimicrobial peptides by rational combinatorial design and high-throughput screening: the importance of interfacial activity, J. Am. Chem. Soc. 131 (2009) 7609-7617.

[98] P.W. Chen, C.L. Shyu, F.C. Mao, Antimicrobial activity of short hydrophobic and basic-rich peptides, Am. J. Vet. Res. 64 (2003) 1088-1092.

[99] A. Wessolowski, M. Bienert, M. Dathe, Antimicrobial activity of arginine and tryptophan rich hexapeptides: the effects of aromatic clusters, D-amino acid substitution and cyclization, J. Pept. Res. 64 (2004) 159-169.

[100] R. Gopal, Y.J. Kim, C.H. Seo, K.S. Hahm, Y. Park, Reversed sequence enhances antimicrobial activity of a synthetic peptide, J. Pept. Sci. 17 (2011) 329–334.

[101] B. Deslouches, S.M. Phadke, V. Lazarevic, M. Cascio, K. Islam, R.C. Montelaro, T.A. Mietzner, De novo generation of cationic antimicrobial peptides: influence of length and tryptophan substitution on antimicrobial activity, Antimicrob. Agents Chemother. 49 (2005) 316-322.

[102] A. Makovitzki, Y. Shai, pH-Dependent antifungal lipopeptides and their plausible mode of action, Biochemistry 44 (2005) 9775-9784.

[103] S. Vylkova, N. Nayyar, W. Li, M. Edgerton, Human β-defensins kill *Candida albicans* in an energy-dependent and salt-sensitive manner without causing membrane disruption, Antimicrob. Agents Chemother. 51 (2007) 154-161.

[104] J.I. Ibeas, H. Lee, B. Damsz, D.T. Prasad, J.M. Pardo, P.M. Hasegawa, R.A. Bressan, M.L. Narasimhan, Fungal cell wall phosphomannans facilitate the toxic activity of a plant PR-5, Plant J. 23 (2000) 375-383.

[105] N.L. Van der Weerden, R.E.W. Hancock, M.A. Anderson, Permeabilization of fungal hyphae by the plant defensin NAD1 occurs through a cell wall dependent process, J. Biol. Chem. 285 (2010) 37513-37520.

[106] D.G. Lee, D.H. Kim, Y. Park, H.K. Kim, Y.K.Shin, C.H. Choi, K.S. Hahm, Fungicidal effect of antimicrobial peptide, PMAP-23, isolated from porcine myeloid against candida albicans, Biochem. Biophys. Res. Commun. 282 (2001) 570-574.

[107] D.G. Lee, P.I. Kim, Y. Park, E.R. Woo, J.S. Choi, C.H. Choi, K.S. Hahm, Design of novel peptide analogs with potent fungicidal activity, based on PMAP-23 antimicrobial peptide isolated from porcine myeloid, Biochem. Biophys. Res. Commun. 293 (2002) 231-238.

[108] C.L. Friedrich, D. Moyles, T.J. Beveridge, R. E. Hancock. Antibacterial action of structurally diverse cationic peptides on Gram-positive bacteria. Antimicrob.

Agents Chemother. 44 (2000) 2086–2092.

[109] J. Lee, C. Park, S.C. Park, E.R. Woo, Y. Park, K.S. Hahm, D.G. Lee, Cell selectivity-membrane phospholipids relationship of the antimicrobial effects shown by pleurocidin enantiomeric peptides, J. Pept. Sci. 15 (2009) 601-606.

[110] J. Lee, D.G. Lee, Antifungal properties of a peptide derived from the signal peptide of the HIV-1 regulatory protein, Rev, FEBS Lett. 583 (2009)1544-1547.

[111] G. Kragol, R. Hoffmann, M.A. Chattergoon, S. Lovas, M. Cudic, P. Bulet, B.A. Condie, K.J. Rosengren, L.J. Montaner, L. Otvos, Identification of crucial residues for the antibacterial activity of the proline-rich peptide, pyrrhocoricin, Eur. J. Biochem. 269 (2002) 4226-4237.

[112] C.B. Park, K.S. Yi, K. Matsuzaki, M.S. Kim, S.C. Kim, Structure-activity analysis of buforin II, a histone H2A-derived antimicrobial peptide: the proline hinge is responsible for the cell-penetrating ability of buforin II, Proc. Natl. Acad. Sci. USA 97 (2000) 8245-8250.

[113] M.I.A. van der Kraan, J. van Marle, K. Nazmi, J. Groenink, W. Van't Hof, E.C.I. Veerman, J.G.M. Bolscher, A.V.N. Arnerongen, Ultrastructural effects of antimicrobial peptides from bovine lactoferrin on the membranes of *Candida albicans* and *Escherichia coli*, peptides 26 (2005) 1537-1542.

[114] E. Vives, P. Brodin, B. Lebleu, A truncated HIV-1 Tat protein basic domain rapidly translocates through the plasma membrane and accumulates in the cell nucleus, J. Biol. Chem. 272 (1997) 16010-16017.

[115] D.J. Schibli, L.T. Nguyen, S.D. Kernaghan, O. Rekdal, H.J. Vogel, Structure-function analysis of tritrpticin analogs: potential relationships between antimicrobial activities, model membrane interactions, and their micelle-bound NMR Structures, Biphys. J. 91 (2006) 4413-4423.

[116] M. Mano, A. Henriques, A. Paiva, M. Prieto, F. Gavilanes, S. Simões, M.C. Pedroso de Lima, Cellular uptake of S413-PV peptide occurs upon conformational changes induced by peptide-membrane interactions, Biochem. Biophys. Acta. (1758) 2006 336-346.

[117] M. Mano, A. Henriques, A. Paiva, M. Prieto, F. Gavilanes, S. Simões, M.C. de Lima, Interaction of S413-PV cell penetrating peptide with model membranes: relevance to peptide translocation across biological membranes, J. Pept. Sci. 13 (2007) 301-313.

[118] S.T. Henriques, M.N. Melo, M.A.R.B. Castanho, cell penetrating peptides and antimicrobial peptides: how different are they, Biochem. J. 399 (2006) 1-7.

[119] W.C. Wimley, K. Hristova, S. ladokhin, L. Silvestro, P.H. Axelsen, S.H. White, Folding of beta sheet membrane proteins: a hydrophobic hexappetide model, J. Mol. Biol 277 (1998) 1091-1110.

[120] A.S. Ladokhin, S.H. White, Folding of amphipathic alpha-helices on membranes: energetics of helix formation by melittin, J. Mol. Biol. 285 (1999) 1363-1369.

[121] H.N. Hunter, W. Jing, D.J. Schibli, T. Trinh, I.Y. Park, S.C. Kim, H.J. Vogel, The interactions of antimicrobial peptides derived from lysozyme with model membrane systems, Biochem. Biophys. Acta 1668 (2005) 175-189.

[122] A.J. Rezansoff, H.N. Hunter, W. Jing, I.Y. Park, S.C. Kim, H.J. Vogel, Interactions of the antimicrobial peptide Ac-FRWWHR-NH_2 with model membrane systems and bacterial cells, J. Pept. Res. 65 (2005) 491-501.

[123] A. Yonezawa, J. Kuwahara, N. Fujii, Y. Sugiura, Binding of Tachyplesin-I to DNA revealed by footprinting analysis-significant contribution of secondary structure to DNA-binding and implication for biological action, Biochemistry 31 (1992) 2998-3004.

[124] C. Subbalakshmi, N. Sitaram, Mechanism of antimicrobial action of indolicidin, FEMS Microbiol. Lett. 160 (1998) 91-96.

[125] H. Ulvatne, O. Samuelsen, H.H. Haukland, M. Kramer, L.H. Vorland, Lactoferricin B inhibits bacterial macromolecular synthesis in *Escherichia coli* and *Bacillus subtilis*, FEMS Microbiol. Lett. 237 (2004) 377-384.

[126] A. Muñoz, B. López-Garcia, J.F. Marcos, Studies on the mode of action of the antifungal hexapeptide PAF26, Antimicrob. Agents Chemother. 50 (2006) 3847-3855.

Abstract

Lysine and tryptophan-rich sequences have been identified in cationic antimicrobial peptides with broad spectrum activity against microbes. I synthesized a series of scrambled peptides containing repeat pattern of lysine (K) and tryptophan (W) residues, $(KW)_n$ (where *n* equals 2, 3, 4 or 5) and determined their antimicrobial activity.

Initially, the effects of linear peptides on bacterial membrane were studied. Increase of chain length led to enhance antibacterial activity of these peptides except for $(KW)_5$ peptide. Reduced antibacterial activity and increased cytotoxicity of $(KW)_5$ peptide were demonstrated to correlate the increased hydrophobicity upon self-aggregation in aqueous environment. The interaction of the peptides with the phosphate groups of lipopolysaccharides (LPS) correlates with their ability to permeate it. Their killing actions were achieved through a rapid collapse of transmembrane potential and an induction of membrane permeability. The present study further indicated the peptides mode of action with negatively charged membranes suggests an aggregation dependent mechanism. Circular dichroism (CD) spectra revealed that these peptides had an unordered structure in aqueous solution, but adopted β-sheet conformation in model lipid vesicles. Finally, $(KW)_4$ peptide disrupted the bacterial cell surface and cells were aggregated, observed by scanning electron microscopy. All data supported that the clustering of KW motifs in longer peptides (*n* equals 4 or 5) contributed to their bactericidal action, although the antibacterial, hemolytic, LPS binding affinity and membrane permeable activities of these peptides were responsible for their chain length, hydrophobicity, solubility and aggregation state.

On the second studies, the effects of peptides on fungal membrane were determined. Antifungal activity of these peptides was increased with their chain length, a similar trend was observed for cytotoxicity. Minimum inhibitory concentration (MIC)

of these peptides did not induce cell permeation but killed fungal pathogens, although antifunal activity was not inhibited by cell wall components and metabolic inhibitor. Membrane integrity was evaluted by extracellular/intracellular accumulation ratio of propidium iodide vs calcein, suggesting that peptide did not caused membrane permeation. Trp blue shift and CD spectra measurements were shown that peptides interacted with fungal membrane, however, their binding on membrane did not induce permeabilization of the cytoplsamic membrane in *C. albicans* at the MIC of the peptide. Scanning electron microscopy (SEM) observation showed no morphological alternation at MIC of $(KW)_4$ peptide. TAMRA-labeled $(KW)_4$ was localized into cytosol of *C. albicans*, interestingly, gel retardation assays suggested that peptide interacted with fungal RNA. The proposed mechanisms by which $(KW)_4$ peptide are able to enter the cytoplasm of *C. albicans* and then the growth inhibition of fungal cells was followed by nucleic acid binding.

Curriculum vitae

Name: Ramamourthy Gopal

Address:

Chosun University, 375 Seosuk-Dong, Dong-Ku, Gwangju, Republic of Korea

Telephone: +82-62-230-6750

E. mail: ramagopa@gmail.com

Personal profile

Date of Birth: October 09, 1978

Gender: Male

Educational and research experiences

1995-1998: B.SC in Biochemistry, South India Vaniar Educational Trust, affiliated to University of Madrass, Gowrivakkam, Chennai, India.

2000-2002: M.SC in Biochemistry, J.J. College of Arts and Science, affiliated to Bharathidasan Univeristy, Pudukkottai, Tamil Nadu, India. (Advisor: Dr. Udayakumar).

2002-2004: M.Phil in Biochemistry, J.J. College of Arts and Science, affiliated to Bharathidasan Univeristy, Pudukkottai, Tamil Nadu, India. (Internal Advisor: Dr. R. Udayakumar, External advisor: Dr. A. Gnanmani (Central leather research institute, Chennai)).

2004-2005: Research assistant in Department of Biochemistry, All India Institute of Medical Science, New Delhi, India (Under Prof. D.N. Rao).

2006-2007: Senior research fellowship in Department of Biophysics, All India Institute of medical science, New Delhi, India (Under Dr. Sharmistha dey and Prof. T.P. Singh)

2008-2011: Ph.D, Department of Biomaterial, Chosun University, Gwangju, Korea (Advisor: Prof. Kyung-Soo Hahm and Prof. Yoonkyung Park).

Publications

1. **Ramamourthy Gopal**, Yoonkyung Park and Kyung-Soo Hahm, Mode of action of $(KW)_n$ peptides in fungal pathogens. (To be communicated)
2. **Ramamourthy Gopal**, Yoonkyung Park and Kyung-Soo Hahm, Influence of a repetitive pattern of Lysine and Tryptophan on antibacterial activity. (To be communicated)
3. Jong-Kook-Lee, **Ramamourthy Gopal**, Yoonkyung Park, The function and application of Antibiotic Peptides, Appl. Chem. Eng. 22 (2011), 119-124.
4. **Ramamourthy Gopal**, Young Jin Kim, Chang Ho Seo, Kyung-Soo Hahm and Yoonkyung Park, Reversed sequences enhances antimicrobial activity of a synthetic peptide, J. Pept. Sci. **5** (2011) 329-334.
5. Nari Jeong, Jin-Young Kim, Seong Cheol Park, Jong-Kook Lee, **Ramamourthy Gopal**, Suyeon Yoo, Byoung Kwan Son, Joon Soo Hahm, Yoonkyung Park, Kyung Soo-Hahm, Antibiotic and synergistic effect of Leu-Lys rich peptide against antiotic resistant microorganisms isolated from patients with cholelithiasis, Biochem. Biophys. Res. Commun. 399 (2010) 581-586.
6. **Ramamourthy Gopal**, Seong-Cheol Park, Seung Joo Cho, Si Wouk Kim, Peter I. Song, Jae-Woon Nah, Yoonkyung Park, Kyung-Soo Hahm, Effect of Leucine and Lysine substitution on the antimicrobial activity and evaluation

of the mechanism of the HPA3NT3 analog peptide, J. Pept. Sci. 15 (2009) 589-594.

7. **Ramamourthy Gopal** and Rajangam Udayakumar, Enzymatic and Non-Enzymatic Antioxidant Activities of *Enicostemma littorale* in *p*-DAB Induced Hepatocarcinoma in Rats, International Journal of Pharmacology, 4 (2008) 369-375.
8. **Ramamourthy Gopal,** Arumugam Gnanamani, Rajangam Udayakumar, S Sadulla, Enicostemma littorale Blume- A potential hypolipidemic plant, Natural Product Radiance 3 (2004) 401-405.
9. Raghu ram K, Udayakumar R, Sivanesan D, Balasundaram M, Gayathri devi, M and **Gopal R**, Hypolipidemic activity of *Enicostemma littorale* (Root) on *p*- DAB induced hepatotoxicity in male albino rats, Biomedicine 23 (2003) 122-127.

Published abstracts

1. A Gnanamani, **R**. **Gopal**, R. Udayakumar, S. Sadulla, A study on scientific validation of the Indian traditional wound healing agent, Wound Repair Regeneration, 12 (2004), A39-A39(1).
2. R. K. Somvanshi, **R. Gopal**, N. Singh, S. Sharma, S. Dey, T. P. Singh, Design of Specific Anti-inflammatory Agents Using Structure-Based Approach: Crystal structure of complex formed between Phospholipase A2 and Tetrapeptide Inhibitor Dehydro Val-Ala-Arg-Ser, Inflammation Research, 55 (2006) Sup. 2, S124.
3. S. Dey, R. K.Somvanshi, A. Kumar, **R. Gopal**, S. Sharma, T. P. Singh, Structure-based Rational Drug design against Inflammation, Rheumatism and Arthritis, Inflammation Research, 55 (2006) Sup. 2, S106.

Scientific Activities

Oral Presentation

1. **Ramamourthy Gopal,** Yoonkyung Park, Kyung-Soo Hahm, **"**Effects of cationic/hydrophobic integration in antimicrobial peptides of the $(KW)_n$ Series", Young scientist session at 12th Korean Peptide-Protein Symposium, November 21, 2008, Korea. (awarded as young scientist)

Poster Presentations

1. **Ramamourthy Gopal,** Kyung-Soo Hahm, Yoonkyung Park, "Antibacterial activity and their mechanism of action on the bacterial membrane of the peptides with an influence of alternating pattern of K and W residues", 5th International Peptide Symposium in conjunction with 47th Japanese Peptide Symposium, December 4-9, 2010, Kyoto International Conference Center, Kyoto, Japan.
2. **Ramamourthy Gopal,** Kyung-Soo Hahm, Yoonkyung Park, "Antibacterial activity of the peptides with an influence of alternating pattern of lysine and trytophan residues and their mechanism of action against the bacterial membrane", Korean Society for biochemistry and molecular biology , May 17-19, 2010, COEX, Seoul, Korea
3. **Ramamourthy Gopal**, Jae-Woon Nah, Yoonkyung Park, Kyung-Soo Hahm, "Effect of Leucine and Lysine substitution on the antimicrobial activity and evaluation of the mechanism of the HPA3NT3 analog peptide", 3rd Asia-Pacific International Peptide Symposium, November 8-11, 2009, Jeju Island, Korea.
4. **Ramamourthy Gopal,** Seung Joo Cho, Kyung-Soo Hahm, Yoonkyung Park, "Effect of Leucine and Lysine substitution on the antimicrobial activity and

evaluation of the mechanism of the HPA3NT3 analog peptide", 66th Korean Society for biochemistry and molecular biology, May 12-13, 2009, COEX, Seoul, Korea.

5. **Ramamourthy Gopal**, Yoonkyung Park, Kyung-Soo Hahm, "In vitro antibiotic effects of a synthetic all-D antimicrobial peptide against clinically isolated drug resistant strains", The 1st Italy-Korea Symposium on Antimicrobial Peptides, July 24-25, 2008, Seo-Suk Hall, Chosun University, Gwangju, Korea.

Acknowledgements

With deep immense of gratitude, I would like to thank everyone who has been helpful in the successful completion of my Ph.D. study.

It is great pleasure to express my hearty gratitude to my esteemed supervisor, **Professor Kyung Soo-Hahm** at Chosun University for giving his healthy suggestions, constant encouragement, support, kind guidance and care throughout this study. It has been a great opportunity to be part of his team and to work on an exciting topic with a lot of scientific freedom which helped me to complete this Ph.D. study successfully.

It is an honor for me to thank my co-supervisor **Professor Yoonkyung Park**. Her valuable comments, understanding, encouraging, guidance have provided a good basis for the present thesis.

I wish to express my gratitude to **Prof. Song Yub Shin, Prof. Ho Jin You, Prof. Il-Seon Park, Prof. Jae Il Kim** for their encouragement and support in various ways.

I would like to thank **Dr. Seong-Cheol Park** for his scientific discussions and offering time for all these interesting results.

Thanks also to **Dr. Jin Young Kim, Dr. Mohammad Abul Farah, Mr. Jong-kook-Lee, Ms. Yoo Suyeon, Ms. Jin Soon Park, Ms. Jeong Na-Ri, Mr. Hae Gyun Park, Ms. Kim Mi Hyun, Mrs. Hoang Thi Huong, Mr. Hyung Jong Na, Ms. Kim Yoon Jin, Ms. Park Kyung Im, Mr. Shin Sun-Oh, Ms. Kang Eun Ji, Ms. Park Eun Jin, Mr. Kim Myeong Sun** to be my friends and to share my live story with good atmosphere in all the ups and downs during my Ph.D. carrier.

My special thanks to the president and the administrative officers in Research center for proteinaous materials at Chosun University.

I extend my thanks to all the people in the International office and Graduate school at Chosun University for their great help.

I wish to thank **Ms. Sumi Kim**, International Relations Coordinator at Chosun University.

My thanks to Korean teachers in Graduate school at Chosun University.

On a personal level, I would like to thank my parents, my father-in-law, my brother, my sister, my wife and my family members for their continues support on my choices, encouragement and love throughout my academic career.

I convey my thanks to all my friends whom I cannot possibly name individually for their valuable support directly or indirectly and their timely help for completion of this work.

My humble thanks to the almighty God for his everlasting guidance and love.